PERFORMANCE ANALYSIS OF TWO REACTION TURBINES

MICHAEL WALTER WALLACE

PERFORMANCE ANALYSIS OF TWO REACTION TURBINES

by

Michael Walter Wallace
Lieutenant, United States Navy

Submitted in partial fulfillment of
the requirements for the degree of

MASTER OF SCIENCE IN AERONAUTICAL ENGINEERING

from the

NAVAL POSTGRADUATE SCHOOL

December 1966

ABSTRACT

A series of air tests with two different turbines was carried out on the Turbine Test Rig at the Naval Postgraduate School, Monterey, California. This study is primarily concerned with the data reduction and performance analysis of these turbines. Recent changes to the Test Rig are described, and performance predictions for geometrically similar turbines operating with media other than air are also presented.

TABLE OF CONTENTS

LIST OF TABLES

LIST OF ILLUSTRATIONS

TABLE OF SYMBOLS

Symbols

A	Area
a_x	Axial dimension
c_p	Specific heat, constant pressure
F	Force
g	Universal gravitational constant
H	Total enthalpy
h	Static enthalpy
h'	Isentropic static enthalpy
(HP)	Horsepower
J	Conversion factor (778 ft lb/BTU)
k_{is}	Head coefficient
k_e	Leaving loss coefficient
M	Moment
$\dot{m}$	Mass flow rate
N	Revolutions per minute
P	Pressure
R	Universal gas constant
R_M	Mean radius
r	Radial dimension
r*	Theoretical degree of reaction
s	Entropy
T	Temperature

Symbols

T'	Isentropic temperature
U	Peripheral velocity
U^*	Equivalent referred peripheral velocity
V	Absolute velocity
V^*	Equivalent referred absolute velocity
W	Relative velocity
W^*	Equivalent referred relative velocity
$\dot{w}$	Weight flow rate

Greek Letters

α	Absolute flow angle
β	Relative flow angle
γ	Specific heat ratio
Δ	Change (in a property)
δ	Referred pressure
ζ	Loss Coefficient
η	Efficiency
θ	Referred temperature
ξ	Flow restriction factor
ρ	Density
Σ	Summation
Φ	Flow Function
ω	Angular Velocity

Subscripts

A	Axial
AX	Axial force capsule measurement
E	Equivalent
IS	Isentropic
M	Mean
P	Constant Pressure
R	Rotor
S	Stator
T	Total
TH	Theoretical
U	Peripheral
x	Axial
0	Upstream of stator
1	Between stator and rotor
2	Downstream of rotor

1. Introduction.

Turbine applications cover a very wide range of operating regimes. In aerospace applications the turbines must often be small due to severe weight limitations. Also the extremes of the harsh environment impose special conditions such as operation with exotic fluids. In order to achieve the necessary performance these turbines often run at very high rotating speeds and the design tolerances become very critical.

In this light all contributing factors must be carefully examined. Relatively unknown are the effects of axial and radial blade clearances upon turbine performance. Determination of these effects was undertaken by tests on the Turbine Test Rig at the Turbo Propulsion Laboratory, Department of Aeronautics, Naval Postgraduate School, Monterey, California. The unique Turbine Test Rig design provides great latitude in the investigation of turbine performance parameters.

This thesis is concerned with the method of analysis and presentation of results of tests on two different reaction turbines.

Since these tests were run with compressed air the prediction of performance with other media is also presented in this thesis.

Thanks and appreciation are given to Professor Vavra for his valuable guidance and to Mr. L. T. Clark for his willing assistance.

2. Test Installation.

The Turbine Test Rig (TTR) is described in detail by Eckert[1] and to avoid duplication this discussion will be concerned primarily with alterations in the installation since Eckert's work, stator-rotor combinations used, and data measurements.

The installation consists basically of a floating stator housing assembly and a rotor assembly. Air is supplied by an axial compressor through a series of plenum tanks. The inlet air pressure forms the "air cushion" to float the stator assembly. This is accomplished through a labyrinth seal between the inlet manifold and the stator assembly. The rotor assembly consists of the rotor and dynamometer connected by the rotor shaft. The dynamometer is remotely controlled to produce desired load on the rotor.

A schematic of the installation is presented in Fig. 1. All tests included herein were conducted without the hood, thus the turbine exhausted directly into the atmosphere. Three conical screens were installed upstream from the stator nozzle to even out the flow and reduce any radial or tangential velocity component at the stator entrance.

Six Kiel total pressure probes and two total temperature probes are installed downstream from the screens, but still upstream from the stator nozzle. The six Kiel probes are stationed at even intervals around

[1]Eckert, R. H., Performance Analysis and Initial Tests of a Transonic Turbine Test Rig (USNPGS Thesis May 1966) Section 2.

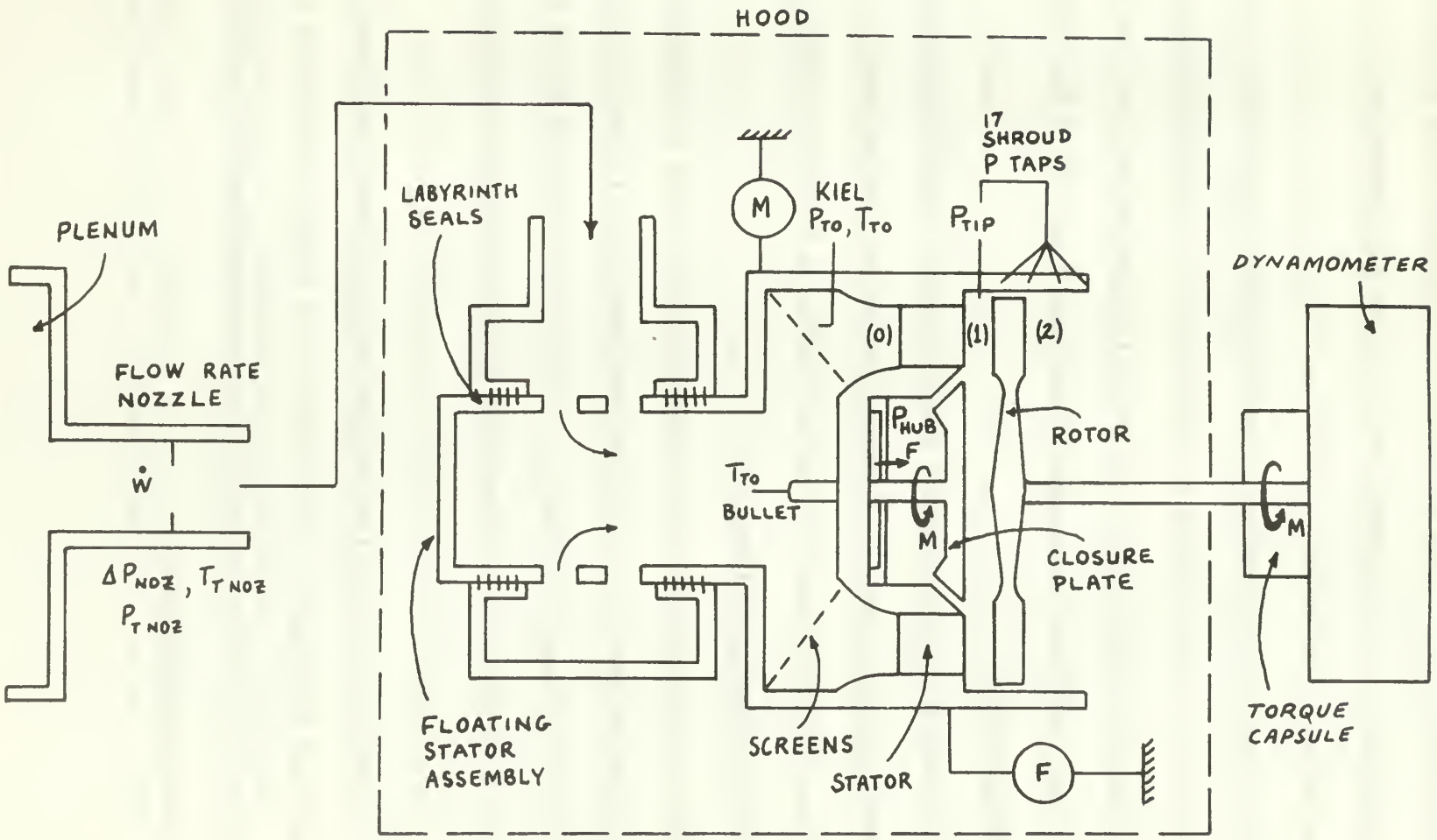

SCHEMATIC OF INSTALLATION - FIGURE 1

the stator assembly circumference, and are averaged to obtain the inlet total pressure P_{TO} . The associated total temperature probes have proven slightly unreliable, therefore the inlet total temperature is taken by the bullet probe indicated in Fig. 1.

The rotor shroud contains seventeen static pressure taps. The extreme upstream tap is taken as the station (1) rotor tip pressure. Proceeding downstream, taps 1-13 are all on the shroud inner perimeter. Taps 14-16 are on the angled bevel and tap 17 is on the extreme end of the shroud.

The station (1) hub pressure is taken from a tap off the stator hub to the chamber between the stator hub and the closure plate. The axial force differential and the moment acting on the closure plate are measured by strain gage flexures.

The main force and moment measurements on the floating stator assembly are measured by the reluctance type force capsules denoted respectively by F and M in Fig. 1. The torque developed by the turbine load is measured by an electronic torque capsule of the dynamometer.

The method of calibration and the set-up of these instruments are described by Eckert.[1] The rotor torque capsule calibration has been refined by a special calibration unit designed to give consistent and repeatable calibrations.

The flow rate measurement method is presented by Eckert.[2] This calibration holds throughout the range of magnitude of flow rates for the tests presented here. For lower flow rates the reader is referred to the work by Naviaux.[3]

A summary of the measurements, which are used in this analysis is given below:

1. The flow rate is calculated from measurements of total temperature, total pressure, and pressure differential across the nozzle, all taken at the flow nozzle. The leakage flow through the labyrinths of the floating stator assembly is obtained from the measured total pressure and total temperature in the plenum and the calibration data of Eckert.[2]

2. On the stator are measured the total inlet temperature, total inlet pressure, hub static pressure, and seventeen shroud static pressures which include the tip static pressure. Direct force measurements include the force and moment on the stator assembly and the force and moment on the closure plate.

3. The rotor measurements are the rotor speed, the torque on the rotor shaft, and the exhaust static pressure.

[2]Eckert, R. H., Determination of Flow Rates, Transonic Turbine Test Rig (USNPGS TN 66T-1 January 1966).

[3]Naviaux, J. C., Transonic Turbine Test Rig Exhauster Tests, and Tests of a Reaction Turbine (USNPGS Thesis Dec. 1966).

The two turbines used in these tests are markedly different in appearance. The so-called MOD I turbine has an outer diameter of approximately 9.9 inches with a blade height of about 1.8 inches. The turbine was designed for free vortex flow and the rotor blades therefore have considerable twist between the hub and tip. The blading at the hub is of the impulse type whereas at the tip it has a degree of reaction of about fifty percent. The blades are fairly thin, and because of the high degree of twist, this rotor is difficult to manufacture. Blade stresses are high and the natural frequencies of the blades are close to the frequencies that the turbine produces. The rotor has 22 blades. The stator of the MOD I turbine has 13 blades which are slightly twisted. The small number of blades became necessary because of the stresses in the blades at the actual operating conditions.

The MOD II turbine has stator and rotor blades that are not twisted. The degree of reaction at the mean diameter is equal to that of the MOD I turbine. The blades have blunt leading edges to become insensitive to the incidence angle variations that occur. The large blade thickness allows cooling holes radially down the center of the blades. However, blade cooling has not been used to date on this turbine. The rotor has 18 blades, a hub diameter of 6.600 inches, and a tip diameter of 9.837 inches. The stator of the MOD II turbine has 19 blades, a hub diameter of 6.795 inches, and a tip diameter of 9.701 inches.

3. Turbine Performance Analysis

The method used for the turbine performance analysis is a one-dimensional approach based on the equations of continuity, energy, momentum, and moment of momentum. The basic approach is that given by Vavra.[4] The assumptions made in conducting the analysis are:

1. The flow is axisymmetric with no initial peripheral component and no radial component throughout.

2. The flow is steady and adiabatic, thus along the mean streamline there is no change in the relative total enthalpy through the rotor.

3. The fluid (air) acts as an ideal gas with constant specific heat throughout the test temperature range.

Conditions across the stator are intended to be found by applying the momentum equation to axial force measurements taken on the floating stator assembly and by applying moment of momentum to the torque measurements. For this case the momentum equation is:

$$\sum F_A = F_{AX} + F_1 - F_2 - F_3 - F_4 - F_5 - F_6 = \dot{m} V_{A1} \qquad (1)$$

where F_{AX} and F_6 are measured by force pickups and the forces F_1 to F_5 are computed from known pressures acting on respective areas.

[4] Vavra, M. H., Aero-Thermodynamics and Flow in Turbo-Machines. New York, London: John Wiley and Sons, Inc., 1960, Chapter 15.

The moment of momentum equation is:

$$\sum M = M_0 + M_6 = \dot{m} R_M V_{U1} \tag{2}$$

where M_0 is measured by a force pickup acting through a known lever arm (actually calibrated for torque). The application of these forces and moments is shown in Fig. 2. The torque M_6 is caused by frictional force due to rotating air between the rotor hub and the closure plate. In Fig. 2 all forces and moments are shown as external forces and are taken as positive values in the directions shown. With the measured weight flow rate $\dot{w}$ there are

$$V_{A1} = \frac{g \sum F_A}{\dot{w}} \tag{3}$$

$$V_{U1} = \frac{g \sum M}{\dot{w} R_M} \tag{4}$$

The equation of continuity can also be used to determine V_{A1}, since

$$V_{A1} = \frac{\dot{w}}{g \rho_1 A_S} \tag{5}$$

The equations of state and energy give

$$\rho_1 = \frac{P_1}{R T_1} \tag{6}$$

$$T_1 = T_{TO} - \frac{V_1^2}{2 g J c_p} \tag{7}$$

D_1	APPROX. 10.9"
D_2	9.867" - 9.905"
D_3	9.702"
D_4	6.798"

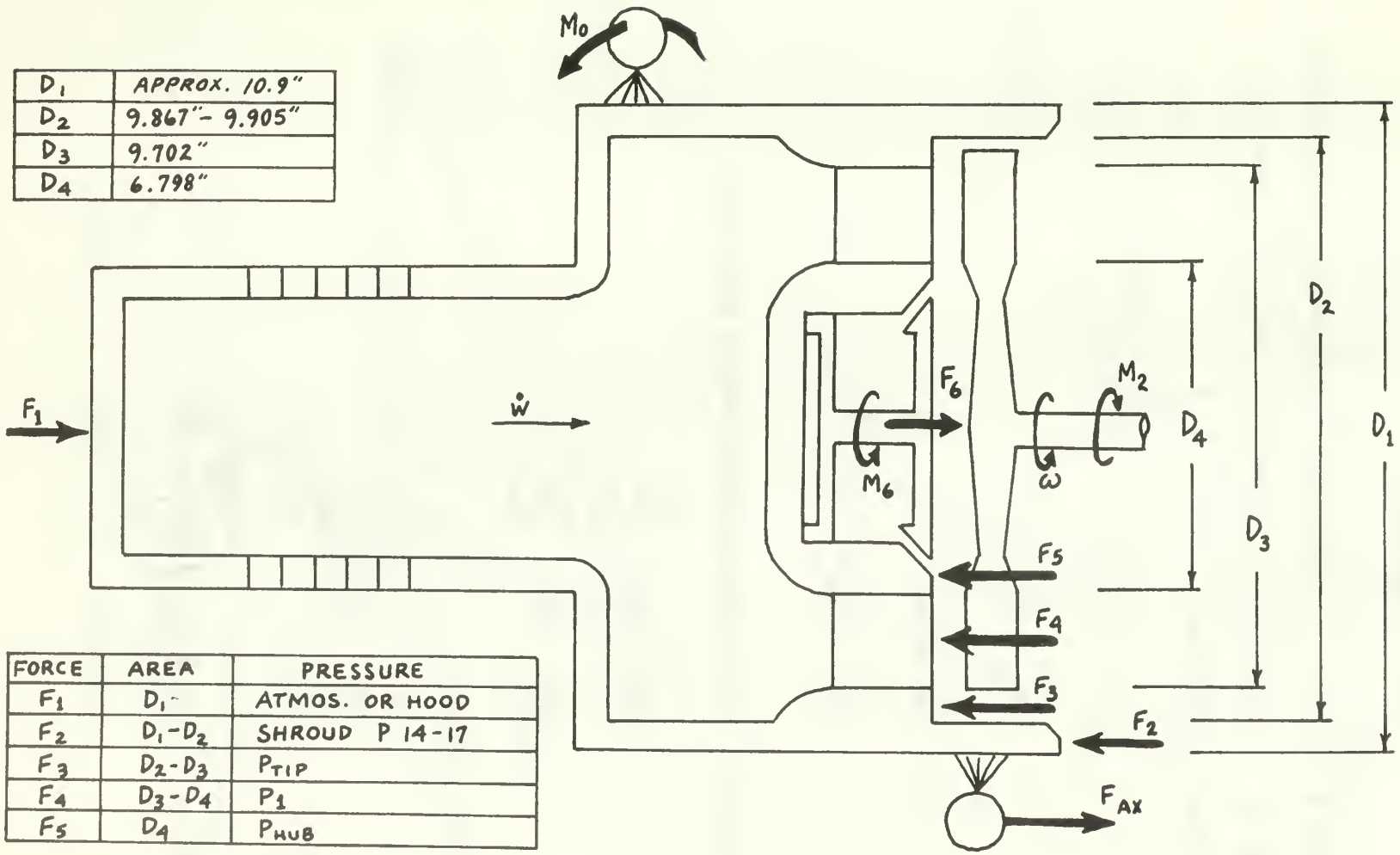

FORCE	AREA	PRESSURE
F_1	D_1	ATMOS. OR HOOD
F_2	$D_1 - D_2$	SHROUD P 14-17
F_3	$D_2 - D_3$	P_{TIP}
F_4	$D_3 - D_4$	P_1
F_5	D_4	P_{HUB}

STATOR ASSEMBLY FORCE DIAGRAM - FIGURE 2

where

$$V_1 = \left(V_{A1}^2 + V_{U1}^2 \right)^{1/2} \tag{8}$$

Equations (5), (6), (7) and (8) may be iterated or solved directly since P_1 is measured. From Fig. 4 additional stator exit quantities are given by

$$U_1 = \omega R_M \tag{9}$$

$$W_{U1} = V_{U1} - U_1 \tag{10}$$

$$W_{A1} = V_{A1} \tag{11}$$

$$W_1 = \left(W_{A1}^2 + W_{U1}^2 \right)^{1/2} \tag{12}$$

The absolute and relative discharge angles are

$$\alpha_1 = \tan^{-1} \frac{V_{U1}}{V_{A1}} \tag{13}$$

$$\beta_1 = \tan^{-1} \frac{W_{U1}}{W_{A1}} \tag{14}$$

The stator efficiency is

$$\eta_S = \frac{T_{TO} - T_1}{T_{TO} - T_{1IS}} \tag{15}$$

where

$$T_{1IS} = T_{TO} \left(\frac{P_1}{P_{TO}} \right)^{(\gamma-1)/\gamma} \tag{16}$$

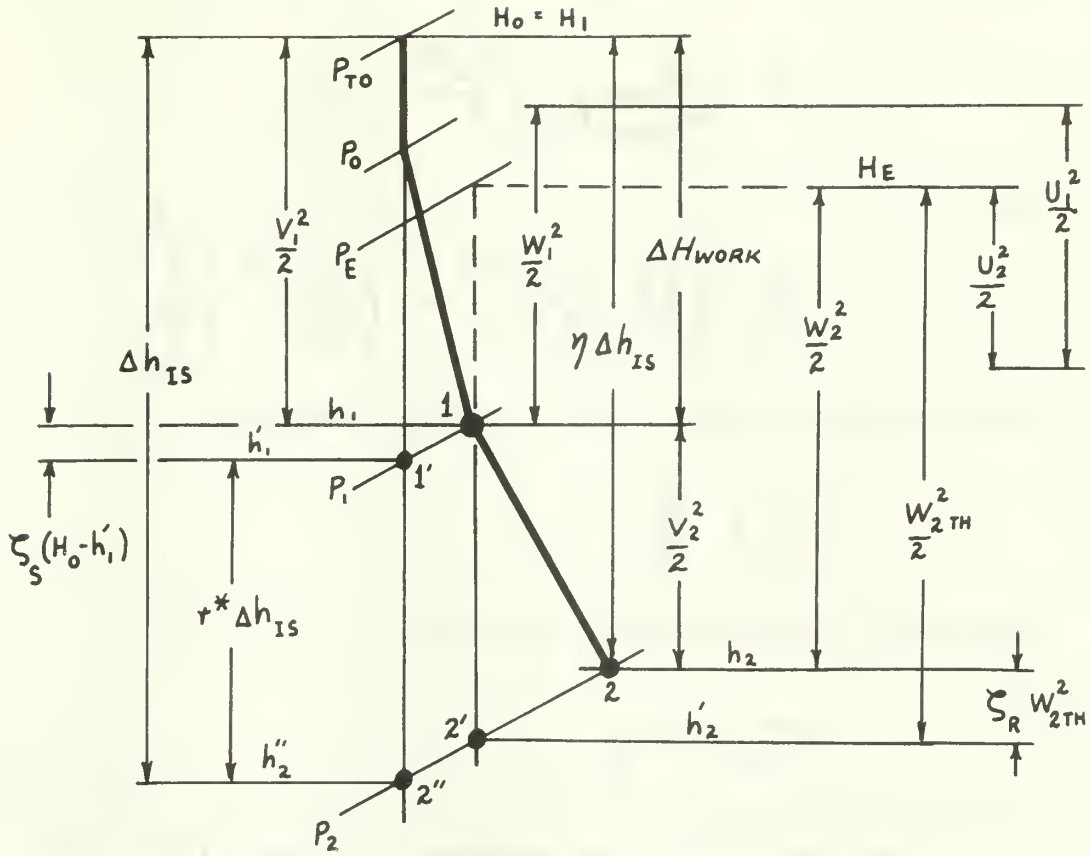

FIGURE 3 h-s DIAGRAM

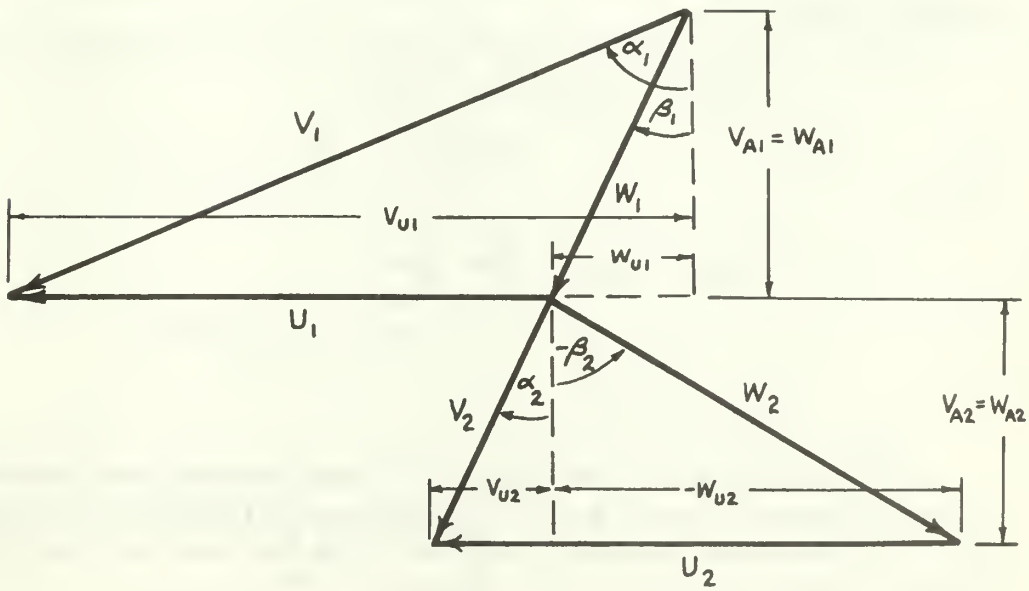

FIGURE 4 VELOCITY DIAGRAM

The flow function Φ is given by Vavra[5] as

$$\Phi = \frac{\dot{w}}{A_{THROAT}\, P_{TO}} \sqrt{\frac{T_{TO}\, R}{g}} \tag{17}$$

and

$$\Phi_{IS} = \left\{ \frac{2\gamma}{\gamma - 1} \left[\left(\frac{P_1}{P_{TO}} \right)^{2/\gamma} - \left(\frac{P_1}{P_{TO}} \right)^{(\gamma+1)/\gamma} \right] \right\}^{1/2} \tag{18}$$

A flow restriction factor ξ_S can then be defined by

$$\xi_S = \frac{\Phi}{\Phi_{IS}} \tag{19}$$

The stator loss coefficient is given by

$$\zeta_S = 1 - \eta_S \tag{20}$$

Conditions at the rotor discharge are found by use of the moment of momentum equation. The torque M_2 measured by the dynamometer is

$$M_2 = \dot{m}\, R_M \left(V_{U1} - V_{U2} \right) \tag{21}$$

Thus

$$V_{U2} = V_{U1} - \frac{g}{\dot{w}} \frac{M_2}{R_M} \tag{22}$$

[5] Vavra, M. H., Problems of Fluid Mechanics in Radial Turbomachines Parts I & II. Von Karman Institute Course Note 55a. Rhode-Saint-Genese, Belgium: Von Karman Institute for Fluid Dynamics, March 1965, equation C (7).

From continuity the axial component is

$$V_{A2} = \frac{\dot{w}}{g \rho_2 A_R} \tag{23}$$

The equations of state and energy give

$$\rho_2 = \frac{P_2}{R T_2} \tag{24}$$

$$T_2 = T_{T2} - \frac{V_2^2}{2 g J c_p} \tag{25}$$

with

$$V_2 = \left(V_{A2}^2 + V_{U2}^2 \right)^{1/2} \tag{26}$$

In order to solve equations (23), (24), (25), (26) either by iteration or directly the values of P_2 and T_{T2} must first be determined. The static pressure P_2 is taken as the static pressure in the exhaust hood or as atmospheric when the hood is not used. Since no energy is removed from the fluid prior to entering the rotor, T_{T2} is found by

$$T_{T2} = T_{T0} - \frac{g}{\dot{w}} \frac{\Delta (\text{POWER})}{2 g J c_p} \tag{27}$$

where

$$\Delta (\text{POWER}) = \omega M_2 \tag{28}$$

The above equations may now be solved to obtain the values of V_{A2}, V_{U2}, and V_2. The peripheral rotor velocity is

$$U_2 = \omega R_M \tag{29}$$

The relative velocities are then determined by

$$W_{U2} = V_{U2} - U_2 \tag{30}$$

$$W_{A2} = V_{A2} \tag{31}$$

$$W_2 = (W_{A2}^2 + W_{U2}^2)^{1/2} \tag{32}$$

The exit flow angles are given by

$$\alpha_2 = \tan^{-1} \frac{V_{U2}}{V_{A2}} \tag{33}$$

$$\beta_2 = \tan^{-1} \frac{W_{U2}}{W_{A2}} \tag{34}$$

The total-to-static efficiency η is defined by Fig. 3 and given by the relation

$$\eta = \frac{T_{TO} - T_{T2}}{T_{TO} - T_{2TH}} \tag{35}$$

where T_{T2} is given by (27). The temperature T_{2TH} is obtained from

$$T_{2TH} = T_{TO} \left(\frac{P_2}{P_{TO}}\right)^{(\gamma-1)/\gamma} \tag{36}$$

The isentropic head coefficient is

$$k_{IS} = \frac{\Delta h_{IS}}{U_1^2/2gJ} = \frac{2gJc_p (T_{TO} - T_{2TH})}{U_1^2} \tag{37}$$

Referred performance values are determined with respect to the reference parameters:

$$\theta = T_{TO} / 518.4 \tag{38}$$

$$\delta = P_{TO} / 14.7 \tag{39}$$

where 518.4 °R and 14.7 psia are standard day sea level atmospheric conditions. The referred values are

$$\dot{W}_{REF} = \frac{\dot{w}\sqrt{\theta}}{\delta} \tag{40}$$

$$M_{2\,REF} = \frac{M_2}{\delta} \tag{41}$$

$$(HP)_{REF} = \frac{(HP)}{\delta\sqrt{\theta}} \tag{42}$$

$$N_{REF} = \frac{N}{\sqrt{\theta}} \tag{43}$$

The theoretical degree of reaction is

$$r^* = \frac{T_{1TH} - T_{2TH}}{T_{TO} - T_{2TH}} \tag{44}$$

Degree of reaction is also determined at the rotor blade hub and tip by

$$r^* = \frac{\left(\frac{P_1}{P_2}\right)^{(\gamma-1)/\gamma} - 1}{\left(\frac{P_{TO}}{P_2}\right)^{\gamma-1/\gamma} - 1} \tag{45}$$

where P_1 is that measured at the hub and the tip respectively. The rotor loss coefficient is

$$\zeta_R = 1 - \frac{W_2^2}{W_{2TH}^2} \tag{46}$$

where

$$W_{2TH} = \left\{ W_1^2 + 2gJc_p T_1 \left[1 - \left(\frac{P_2}{P_1}\right)^{(\gamma-1)/\gamma} \right] \right\}^{1/2} \tag{47}$$

4. Turbine Tests and Results

Tests analyzed here were made with the MOD I turbine, runs 21 through 38, beginning August 11, 1966, and ending September 10, 1966, and with the MOD II turbine, runs 39 through 47, beginning September 17, 1966, and ending October 18, 1966. The most productive runs were 22, 23, 35, 36, 37, 40, 44 and 45. Many of the other runs were used for the specific purpose of clarifying certain points, testing the installation or making radial surveys at the turbine exhaust. Tables I and II contain a brief summary of the tests, indicating the radial and axial clearances which were investigated.

Prior to each test the measurement systems for stator force and moment, and rotor moment were calibrated. The closure plate force and moment measurement systems were calibrated several times initially but due to small and repeatable readings were not calibrated prior to each run. The thermocouple temperature readings were referenced to ice water at 32^{o} F for each run.

Tests were conducted by setting the inlet total pressure at the desired level and then varying the RPM by varying the load imposed by the dynamometer. Maximum load produced minimum RPM. Since RPM effected inlet total pressure, the inlet total pressure had to be readjusted after each RPM change.

TABLE I

MOD I TURBINE

RUN	Δr INCHES	Δa_x INCHES	P_{To}/P_2
21	0.020	0.150	1.3
22	0.020	0.180	1.3, 1.4, 1.5, 1.55
23	0.020	0.410	1.2, 1.3, 1.4, 1.5, 1.55
24	STATIC TESTS		
25	0.020	0.090	1.4, 1.5
26	0.020	0.620	1.4, 1.5
27	0.020	0.290	1.4, 1.5
28	0.033	0.180	1.5
29	0.033	0.180	1.5
30	0.033	0.180	1.5
31	0.033	0.180	1.5
32	0.033	0.180	1.5
33	0.033	0.180	1.4
34	0.033	0.180	1.5
35	0.033	0.180	1.2, 1.3, 1.4, 1.5, 1.55
36	0.033	0.090	1.3, 1.4, 1.5
37	0.033	0.410	1.3, 1.4, 1.5
38	STATIC TESTS		

TABLE II

MOD II TURBINE

RUN	Δr INCHES	Δa_x INCHES	P_{To}/P_2
39	0.015	0.410	1.5, 1.3
40	0.015	0.410	1.3, 1.4, 1.5
41	0.015	0.410	1.4
42	0.015	0.410	1.5
43	0.015	0.410	1.3, 1.4, 1.5, 1.55
44	0.024	0.410	1.3, 1.4, 1.5, 1.55
45	0.033	0.410	1.3, 1.4, 1.5, 1.55
46	0.033	0.410	1.5
47	0.033	0.410	1.5

The maximum inlet total temperature for these runs was about 127°F, while most of the runs were in the 110°F to 115°F range.

The mean radius used in data reduction was 4.187 inches. This value was obtained from

$$R_M^2 = \frac{\int_{R_i}^{R_o} r^2\, dr}{\int_{R_i}^{R_o} dr} = \frac{1}{3}\left(R_o^2 + R_o R_i + R_i^2\right) \tag{48}$$

The head coefficient is referred to an arbitrary mean radius of 4.125 inches.

In order to obtain the mean static pressure P_1 between the stator and rotor a linear variation was assumed between the hub pressure and the tip pressure, or

$$P_1 = \frac{P_{HUB} + P_{TIP}}{2} \tag{49}$$

The data obtained from these tests was reduced on the CDC 1604 computer of the Naval Postgraduate School with a program incorporating the analysis of the preceeding section. The tabulated results and the computer programs are filed under separate cover at the Turbo-Propulsion Laboratory, Naval Postgraduate School, Monterey, California. Contained in this report are graphic summaries of the results.

The effect of axial clearance between the stator and rotor was investigated through two series of runs with the MOD I turbine. The first series, with a common radial clearance of 0.020 inches, is shown in Fig. 5 . The axial clearance was varied between the extremes of

0.090 inches and 0.620 inches. No clearcut pattern of efficiencies emerges, and the points associated with all axial clearances are quite interspersed. However, the highest efficiency was obtained at the greatest axial clearance, and at the second greatest axial clearance ($\Delta a_x = 0.41$ inches) the lowest efficiency was produced at a head coefficient of about 2.1. If only the optimum efficiency point for each clearance is considered it appears that increasing clearance increases efficiency.

The second series of tests at different axial clearances is shown in Fig. 6, where the common radial clearance is 0.033 inches. Axial clearances varied between 0.090 and 0.410 inches. Again, the results do not point to any clear interdependence of axial clearance and efficiency, but do corroborate the results of the first series. Based on these tests it can be concluded that efficiency is not greatly dependent on axial clearance variation from one percent to six percent of the turbine diameter.

Increasing radial clearance is associated with a decrease in efficiency because of the tip clearance flow. In Fig. 7 are shown the efficiencies of the MOD I turbine at rotor tip clearances of 0.020 inches and 0.033 inches at pressure ratios of 1.3 and 1.5. At both pressure ratios the efficiency decreased by about two points if the radial clearance was increased from 1.1 to 1.8 percent of the mean rotor blade height of 1.82 inches.

Various performance plots of the MOD I turbine are shown in Figs. 8, 9, and 10. Fig. 8 shows that at any particular pressure ratio the torque produced is a nearly linear function of the referred speed. A comparison of this relation at the two different radial clearances yielded no discernable difference except very slight displacement of the 1.5 pressure ratio line. It can be noted that the curves for the different pressure ratios have nearly equal slopes.

The effect of radial clearance upon flow rate becomes evident in Fig. 9. An increase in radial clearance produces an increase in flow rate. As the pressure ratio increases this effect becomes more pronounced. It can also be seen by the slopes of the lines that the referred speed has a greater effect on flow rate at lower pressure ratios.

The power produced by the turbine is a direct function of the pressure ratio as exhibited in Fig. 10. Radial and axial clearance had practically no effect on the power generated, but the larger flow rate that passes through the turbine at increased radial clearances decreases the efficiency.

Since it was shown with the MOD I tests that different axial clearances had a negligible effect on performance the tests with the MOD II turbine were carried out at a fixed axial clearance of 0.410 inches for the three radial tip clearances of 0.015, 0.024, and 0.033 inches. The plots of Figs. 11, 12, 13 and 14 show a consistent drop in efficiency of 2.5 to 3.0 points for an increase in radial clearance from about 1.5 to 2.0 percent of the blade height . This indicates

that at clearances greater than about 1.5 percent of the blade height the efficiency decreases radically.

That referred torque is a linear function of referred speed is again verified by Fig. 15 where it is shown again that radial clearances have no appreciable effect.

The MOD II turbine shows the same tendency as the MOD I turbine as far as the influence of radial clearance on flow rate is concerned. However, Fig. 16 shows that for the MOD II turbine the referred speed has a more pronounced effect on flow rate at low pressure ratios than that obtained for the MOD I turbine.

In contrast to the results with the MOD I stage the radial clearances have an effect on the power produced by the MOD II turbine at all pressure ratios. This effect is clearly shown in Fig. 17 . Moreover, both curves show a slight deviation from the linear relationship between power and pressure ratio, at pressure ratios higher than about 1.5.

The effect of pressure ratio on the efficiency of the MOD II turbine is somewhat surprising. Since the design pressure ratio is about 1.5, the highest efficiency should occur at this value. However, the peak efficiency at radial clearances of 0.024 and 0.033 inches occurred at the lowest pressure ratio as exhibited in Fig. 18. The results of runs 40 and 43 for a radial clearance of 0.015 inches, which are shown in Fig. 19, were more as expected and contrary to

Fig. 18. No feasible explanation can be offered for the difference between Fig. 18 and Fig. 19 without additional test runs.

Fig. 20 summarizes the effect of radial clearance on efficiency for both turbines. The radical decrease in efficiency at radial clearances greater than 1.5 percent of blade height is clearly evident on the MOD II curve. The dashed lines are conjectural and additional runs are necessary for continuation of the curves.

5. Turbine Performance Prediction for Different Fluids

Prediction of the turbine performance for media other than air may be made on the basis of air test results. Similarity laws make it possible to relate air test data to gases with different properties except for the effect of the value of the specific heat ratio γ. To account for this effect a method established by Vavra[6] can be used, of which the highlights are presented here only.

The analysis is based on the conditions that the dimensionless equivalent velocities

$$V_1^* = \frac{V_1}{\sqrt{g R T_1}} \tag{50}$$

and

$$U_1^* = \frac{U_1}{\sqrt{g R T_1}} \tag{51}$$

[6] Vavra, M. H., Determination of Single-Stage Turbine Performance at Various Values of Specific Heat Ratio, Unpublished Notes of 8 August 1966.

at the stator discharge remain equal for operations with air and with a gas having an arbitrary value of γ . Moreover it is assumed that

α_1 = rotor absolute entrance angle

and

β_2 = rotor relative discharge angle

remain unchanged. The following turbine parameters are supposed to be known:

A_S, A_R = stator and rotor throat areas, respectively

ζ_S, ζ_R = stator and rotor loss coefficients, respectively

ξ_S, ξ_R = stator, rotor restriction coefficients referred to throat areas

and the particular specific heat ratio of interest.

For the stator the energy equation gives

$$\frac{T_{T0}}{T_1} = 1 + \frac{\gamma - 1}{2\gamma} \left(V_1^*\right)^2 \tag{52}$$

From Fig. 3 it can be seen that

$$\zeta_S = \frac{(T_{T0} - T_1') - (T_{T0} - T_1)}{(T_{T0} - T_1')} \tag{53}$$

Thus

$$\frac{T_1'}{T_{T0}} = \frac{\frac{T_1}{T_{T0}} - \zeta_S}{1 - \zeta_S} \tag{54}$$

and

$$\frac{P_1}{P_{T0}} = \left(\frac{T_1'}{T_{T0}}\right)^{\gamma/(\gamma-1)} \tag{55}$$

The equivalent flow rate is given by

$$\dot{W}_0^* = \frac{\dot{W}\sqrt{T_{TO}}}{P_{TO}}\sqrt{\frac{R}{g}} = A_S \xi_S \left\{ \frac{2\gamma}{\gamma-1}\left[\left(\frac{P_1}{P_{TO}}\right)^{2/\gamma} - \left(\frac{P_1}{P_{TO}}\right)^{(\gamma+1)/\gamma} \right] \right\}^{1/2} \tag{56}$$

where the limiting case is the choked condition that occurs at a pressure ratio of

$$\left(\frac{P_1}{P_{TO}}\right)_{CRITICAL} = \left(\frac{2}{\gamma+1}\right)^{\gamma/(\gamma-1)} \tag{57}$$

The remaining stator relationships are

$$V_{U1}^* = V_1^* \sin \alpha_1 \tag{58}$$

$$V_{A1}^* = V_1^* \cos \alpha_1 \tag{59}$$

$$W_{U1}^* = V_{U1}^* - U_1^* \tag{60}$$

$$W_1^* = \left[(W_{U1}^*)^2 + (V_{A1}^*)^2 \right]^{1/2} \tag{61}$$

$$\beta_1 = \tan^{-1} \frac{W_{U1}^*}{V_{A1}^*} \tag{62}$$

For the rotor an equivalent temperature is defined such that

$$T_E = T_1 + \frac{W_1^2}{2gJc_p} - \frac{U_1^2 - U_2^2}{2gJc_p} \tag{63}$$

The relationship between U_1 and U_2 is known from the rotor radius ratio R_2/R_1 where R_2 and R_1 are mean rotor radii at discharge and inlet respectively. It follows that

$$\frac{T_E}{T_1} = 1 + \frac{\gamma-1}{2\gamma}\left[(W_1^*)^2 - (U_1^*)^2 \left(1 - \frac{R_2^2}{R_1^2}\right) \right] \tag{64}$$

and

$$\frac{P_E}{P_1} = \left(\frac{T_E}{T_1}\right)^{\gamma/(\gamma-1)} \tag{65}$$

Now

$$\frac{\dot{w}\sqrt{T_E}}{P_E}\sqrt{\frac{R}{g}} = \dot{w}_o^* \frac{\sqrt{T_E/T_{TO}}}{P_E/P_{TO}} = \dot{w}_E^* \tag{66}$$

where T_E/T_{TO} is found from (52) and (64), and P_E/P_{TO} from (55) and (65). The rotor flow function is

$$\Phi_R = \frac{\dot{w}_E^*}{A_R \xi_R} = \left\{\frac{2\gamma}{\gamma-1}\left[\left(\frac{P_2}{P_E}\right)^{2/\gamma} - \left(\frac{P_2}{P_E}\right)^{(\gamma+1)/\gamma}\right]\right\}^{1/2} \tag{67}$$

Since the left side of (67) is known P_2/P_E may be found by iteration where the limiting case is the choked rotor flow, given by

$$\Phi_{CRITICAL} = \left(\frac{2}{\gamma+1}\right)^{1/(\gamma-1)}\sqrt{\frac{2\gamma}{\gamma+1}} \tag{68}$$

Now

$$\frac{T_2}{T_E} = \left(\frac{P_2}{P_E}\right)^{(\gamma-1)/\gamma} \tag{69}$$

and

$$\frac{W_2^2}{2gJc_p} = (1-\zeta_R)(T_E - T_2) \tag{70}$$

Hence

$$(W_2^*)^2 = \frac{2\gamma}{\gamma-1}(1-\zeta_R)\left(\frac{1}{(P_2/P_E)^{(\gamma-1)/\gamma}} - 1\right) \tag{71}$$

Also, from Fig. 4

$$W_{U2}^{*} = W_{2}^{*} \sin \beta_2 \tag{72}$$

$$W_{A2}^{*} = W_{2}^{*} \cos \beta_2 \tag{73}$$

$$V_{U2}^{*} = U_{1}^{*} \sqrt{\frac{T_1}{T_2}} \frac{R_2}{R_1} + W_{U2}^{*} \tag{74}$$

$$\alpha_2 = \tan^{-1} \frac{V_{U2}^{*}}{W_{A2}^{*}} \tag{75}$$

and

$$\frac{P_{TO}}{P_2} = \frac{P_{TO}}{P_1} \frac{P_1}{P_E} \frac{P_E}{P_2} \tag{76}$$

The stage performance characteristics of interest are total-to-static efficiency, isentropic head coefficient, theoretical degree of reaction, and the leaving loss coefficient. The isentropic temperature drop ΔT_{IS} is obtained from

$$\frac{\Delta T_{IS}}{T_{TO}} = 1 - \frac{1}{\left(\frac{P_{TO}}{P_2}\right)^{\frac{(\gamma-1)}{\gamma}}} \tag{77}$$

With Euler's Turbine Equation the work output is

$$\Delta T_{WORK} = \frac{1}{g J c_p} \left(U_1 V_{U1} - U_2 V_{U2}\right) \tag{78}$$

which gives

$$\frac{\Delta T_{WORK}}{T_{TO}} = \frac{\gamma-1}{\gamma} \left[U_1^{*} V_{U1}^{*} \frac{T_1}{T_{TO}} - U_1^{*} \frac{R_2}{R_1} \sqrt{\frac{T_1}{T_{TO}}} \, V_{U2}^{*} \sqrt{\frac{T_2}{T_{TO}}} \right] \tag{79}$$

where T_2/T_{TO} is

$$\frac{T_2}{T_{TO}} = \frac{T_2}{T_E} \frac{T_E}{T_{TO}} \tag{80}$$

The total-to-static efficiency is then

$$\eta = \frac{\Delta T_{WORK}/T_{TO}}{\Delta T_{IS}/T_{TO}} \tag{81}$$

The head coefficient is defined by

$$k_{IS} = \frac{2gJc_p \Delta T_{IS}}{U_1^2} \tag{82}$$

and can be expressed as

$$k_{IS} = \frac{2\gamma}{\gamma-1} \frac{T_{TO}}{T_1} \frac{\Delta T_{IS}/T_{TO}}{(U_1^*)^2} \tag{83}$$

From Fig. 3 the degree of reaction is obtained from

$$r^* \Delta T_{IS} = \Delta T_{IS} - (T_{TO} - T_1') \tag{84}$$

which leads to

$$r^* = \frac{T_1'/T_{TO} + \Delta T_{IS}/T_{TO} - 1}{\Delta T_{IS}/T_{TO}} \tag{85}$$

The leaving loss coefficient is defined as

$$k_e = \frac{V_2^2}{2gJc_p \Delta T_{IS}} \tag{86}$$

or

$$k_e = \frac{\gamma-1}{2\gamma} \left[(W_{A2}^*)^2 + (V_{U2}^*)^2 \right] \frac{T_2/T_{TO}}{\Delta T_{IS}/T_{TO}} \tag{87}$$

A typical prediction on the basis of the preceeding presentation is given in Tables III and IV. The chosen fluid is supposed to have a specific heat ratio of 1.2572. The tables are self-explanatory and contain all input values which result from the air model performance

analysis. The calculations were carried out by electronic digital computer, since various iterations were necessary to determine the performance values at specified pressure ratios.

6. Discussion and Recommendations.

In section 3, two methods were presented for obtaining the stator performance, namely one based on momentum, the other on continuity considerations. For the final results continuity was relied upon. Momentum is the preferable method because of the nature of the instrumentation and reliance upon external, direct measurements. However, momentum produced consistently high axial velocities. This may be due to several factors. First was the attainment of the average pressure P_1 between stator and rotor. The assumption of linearity between the hub and tip did not give the desired results, and attempts of varying P_1 in accordance with other relationships did not produce agreement between momentum and continuity either. Possible reasons for this discrepancy may be due to other factors also, particularly, the difficulties associated with the determination of the exact value of the net axial force produced by the axial component of the stator discharge velocity. For a mass flow rate of about 5 lb_m/sec and an axial velocity at the stator exit of about 240 ft/sec the resultant net force due to momentum change is about 37 lb_f. The axial force measured by the force capsule is about 135 lb_f, and the force exerted on the closure plate is about 30 lb_f. From the difference between these two measurements, namely 105 lb_f,

68 lb_f are produced by pressure distributions that act on the shroud and cross sectional areas at station (1). It is readily seen that a small error in the measured forces produces a large error in the net force and axial velocity. It is necessary also that extreme care be taken in determining the exact pressures acting on particular areas of the stator assembly. It is recommended that instrumentation be introduced through the shroud between the stator and rotor to gain exact pressure and temperature distributions between the hub and tip. This could be done at axial clearances of about 0.4 to 0.6 inches.

Efficiency and power are direct functions of the rotor shaft torque. The readings from the electronic torque capsule seemed somewhat doubtful because a number of calibrations failed to produce exact repeatability, and the calibration curves were not quite linear in several cases. Due to the importance of this measurement it would greatly benefit future data analyses to have this situation rectified.

The present computer program for the data reduction could still be improved considerably. Together with the above mentioned improvements, more exact determinations of the flow restriction factors and the loss coefficients would then be possible. These performance parameters are particularly important for the prediction method of section 5.

An error analysis was begun but not completed. It was planned to feed into the computer program the maximum variations of the readings in such combinations as to produce the maximum possible deviation from the average values. This procedure would be an "actual" error analysis and of more value than a theoretical attempt. Prior solution of the above-mentioned problems would greatly improve the accuracy of this error analysis.

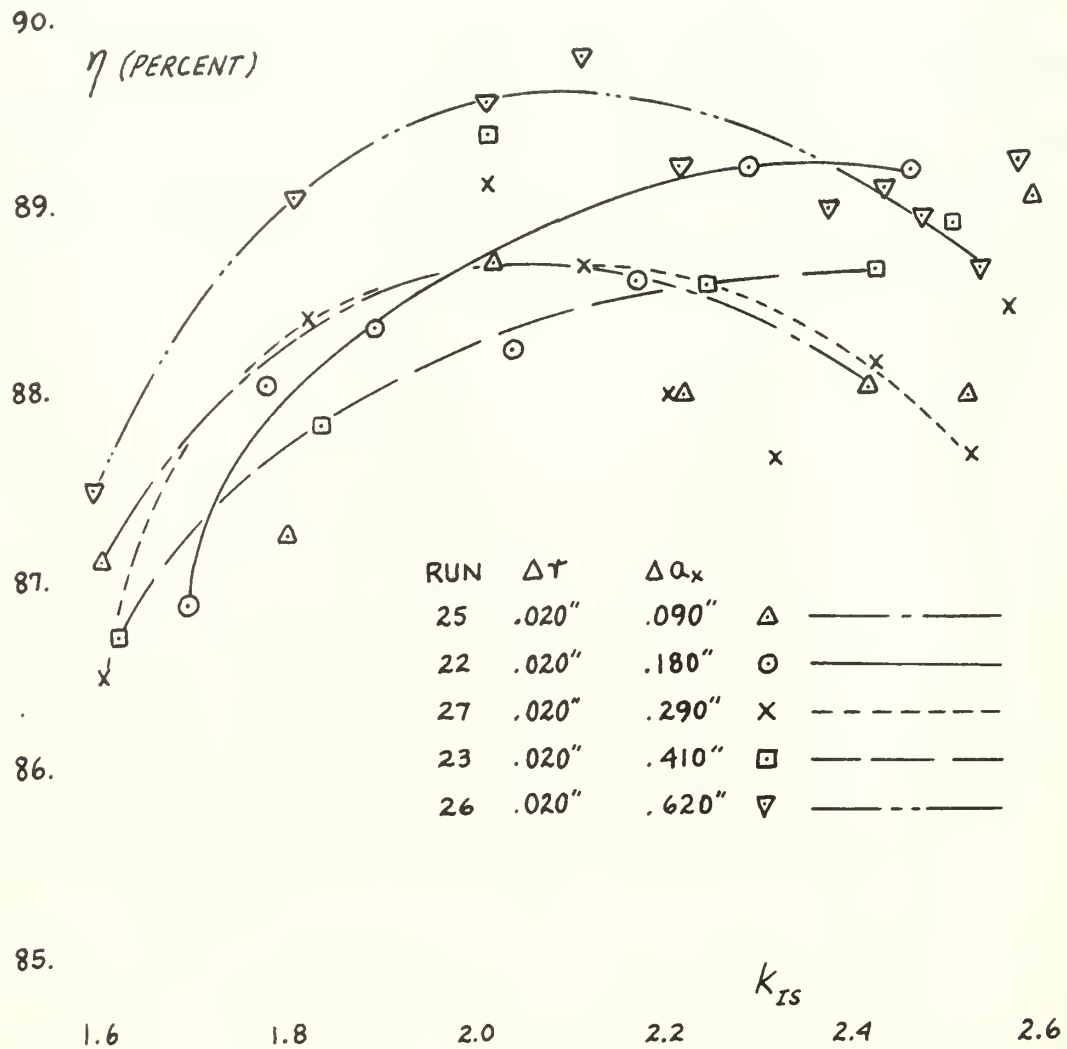

PLOT OF

TOTAL-STATIC EFFICIENCY VS ISENTROPIC HEAD COEFFICIENT

FOR THE MOD I ROTOR

$P_{T0}/P_2 = 1.5$

FIGURE 5

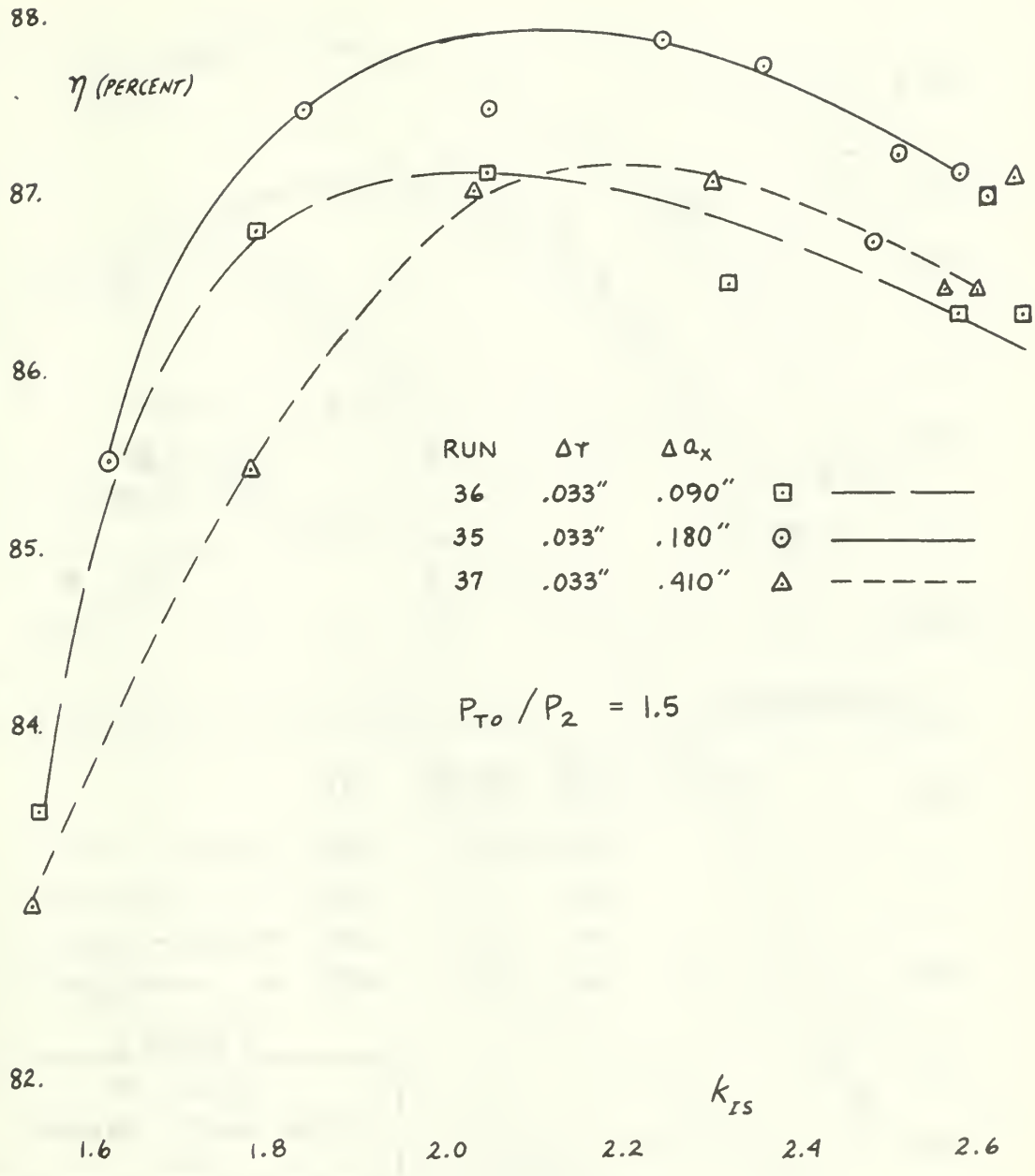

PLOT OF

TOTAL-STATIC EFFICIENCY VS ISENTROPIC HEAD COEFFICIENT FOR THE MOD I ROTOR AT $P_{TO}/P_2 = 1.5$

FIGURE 6

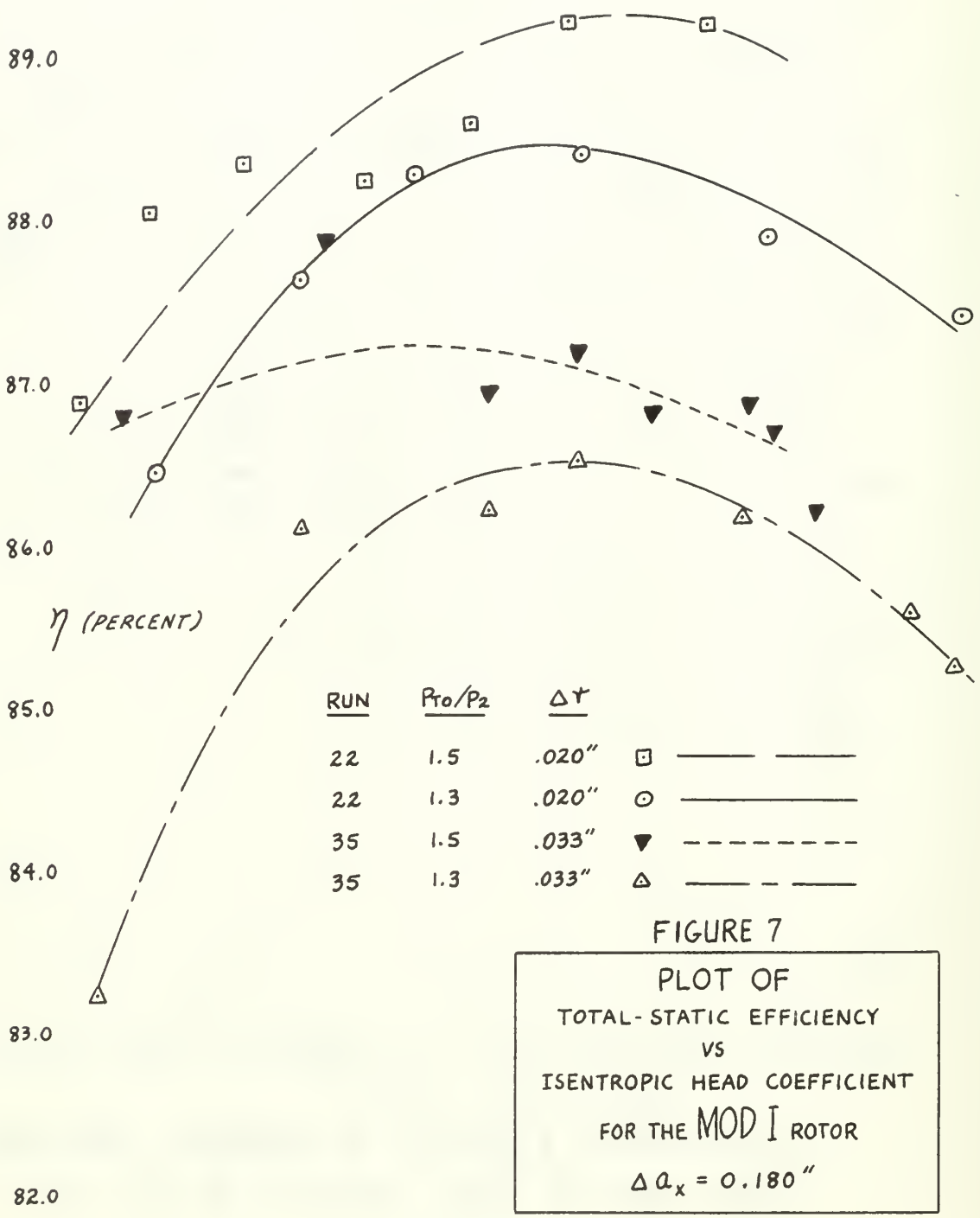

FIGURE 7

PLOT OF
TOTAL-STATIC EFFICIENCY
VS
ISENTROPIC HEAD COEFFICIENT
FOR THE MOD I ROTOR
$\Delta a_x = 0.180"$

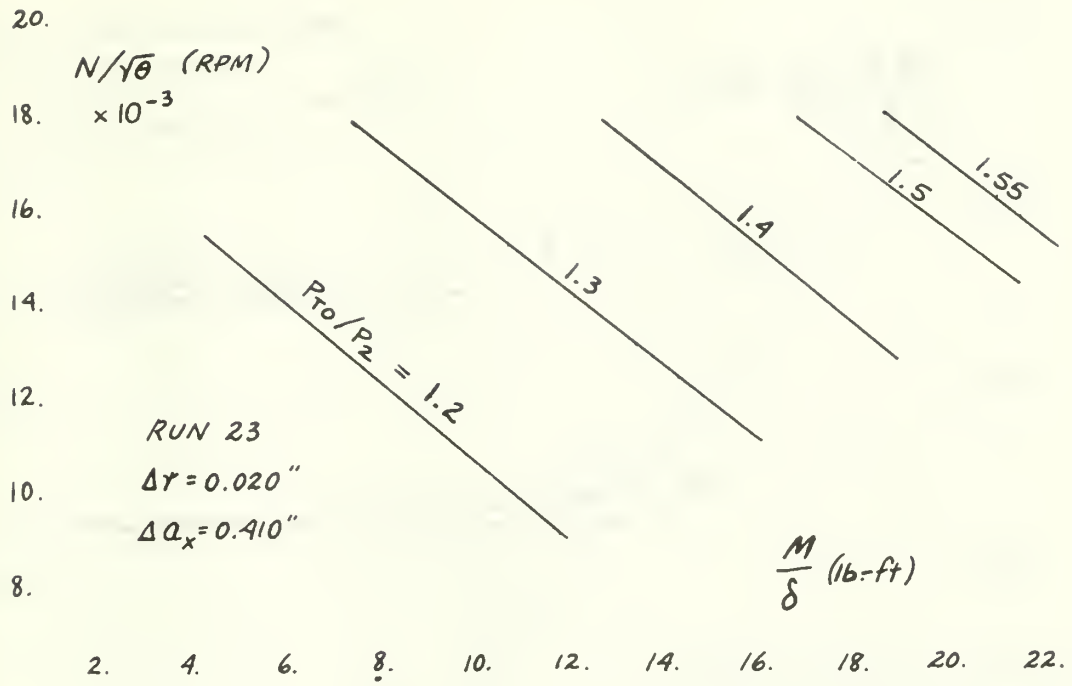

PLOTS OF REFERRED SPEED VS REFERRED TORQUE FOR THE MOD I ROTOR

FIGURE 8

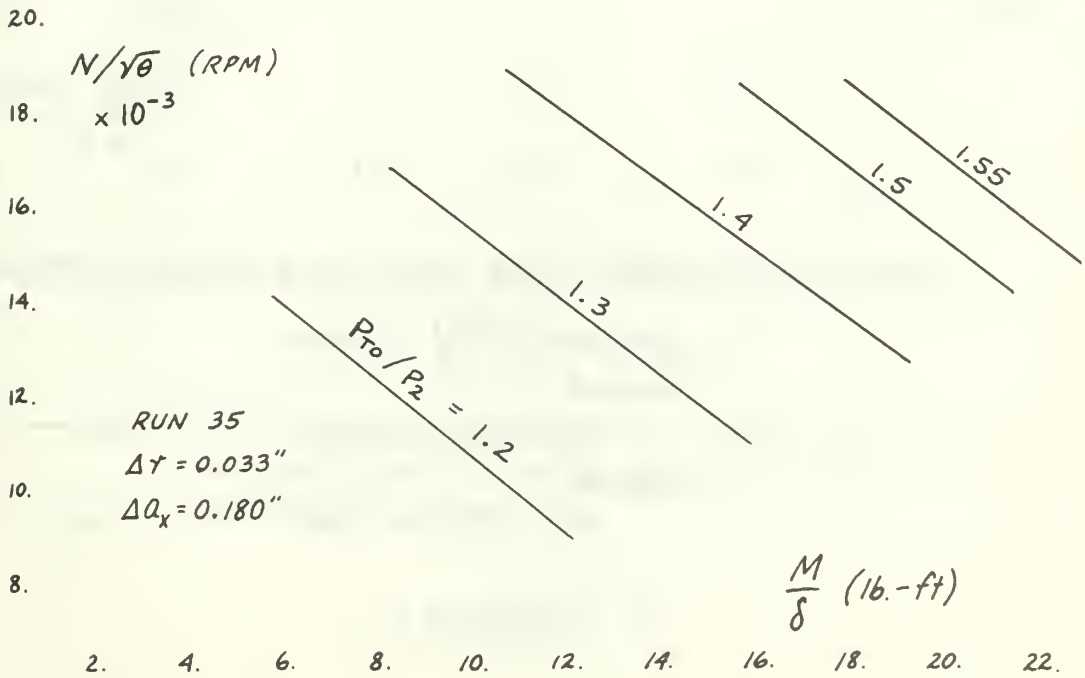

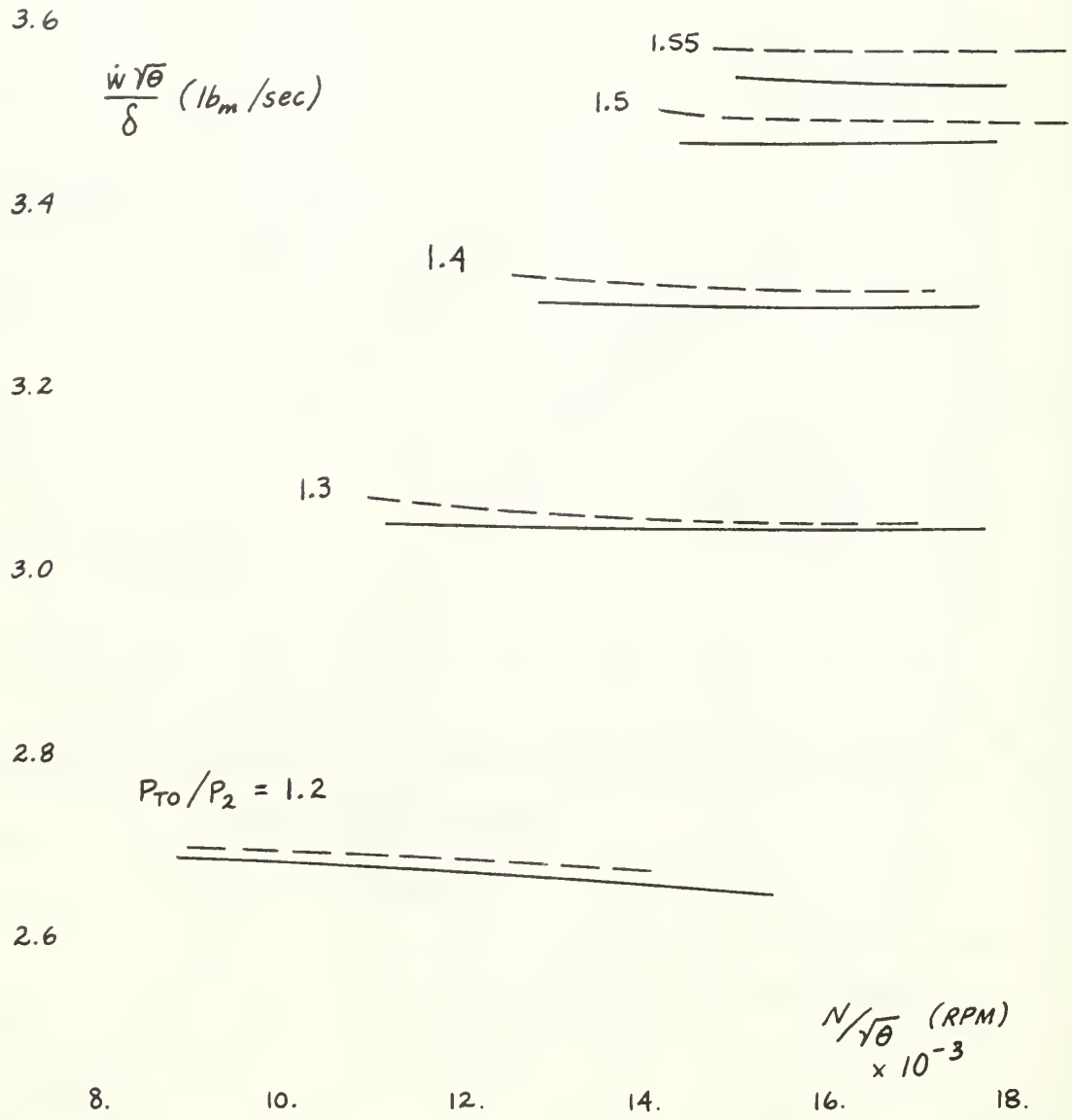

PLOT OF REFERRED FLOW RATE VS REFERRED SPEED

FOR THE MOD I ROTOR

RUN 23

$\Delta r = .020''$, $\Delta a_x = .410''$ ————

RUN 35

$\Delta r = .033''$, $\Delta a_x = .180''$ — — — — —

FIGURE 9

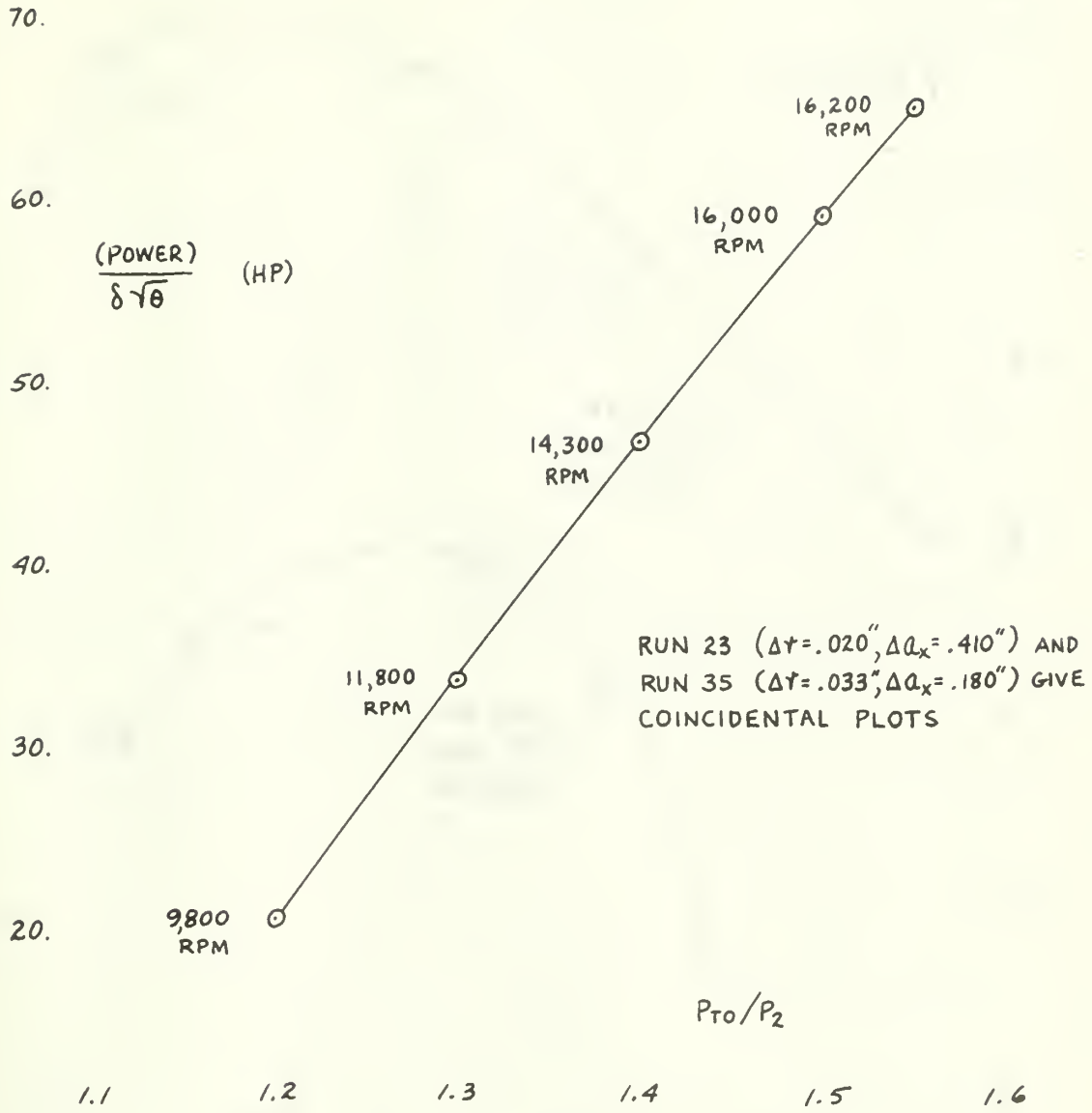

PLOT OF REFERRED POWER VS PRESSURE RATIO
FOR THE MOD I ROTOR

NOTE : "PEAK" POWER AT THE PARTICULAR PRESSURE RATIO IS THE VALUE PLOTTED, AND THE ASSOCIATED RPM IS ALSO INDICATED.

FIGURE 10

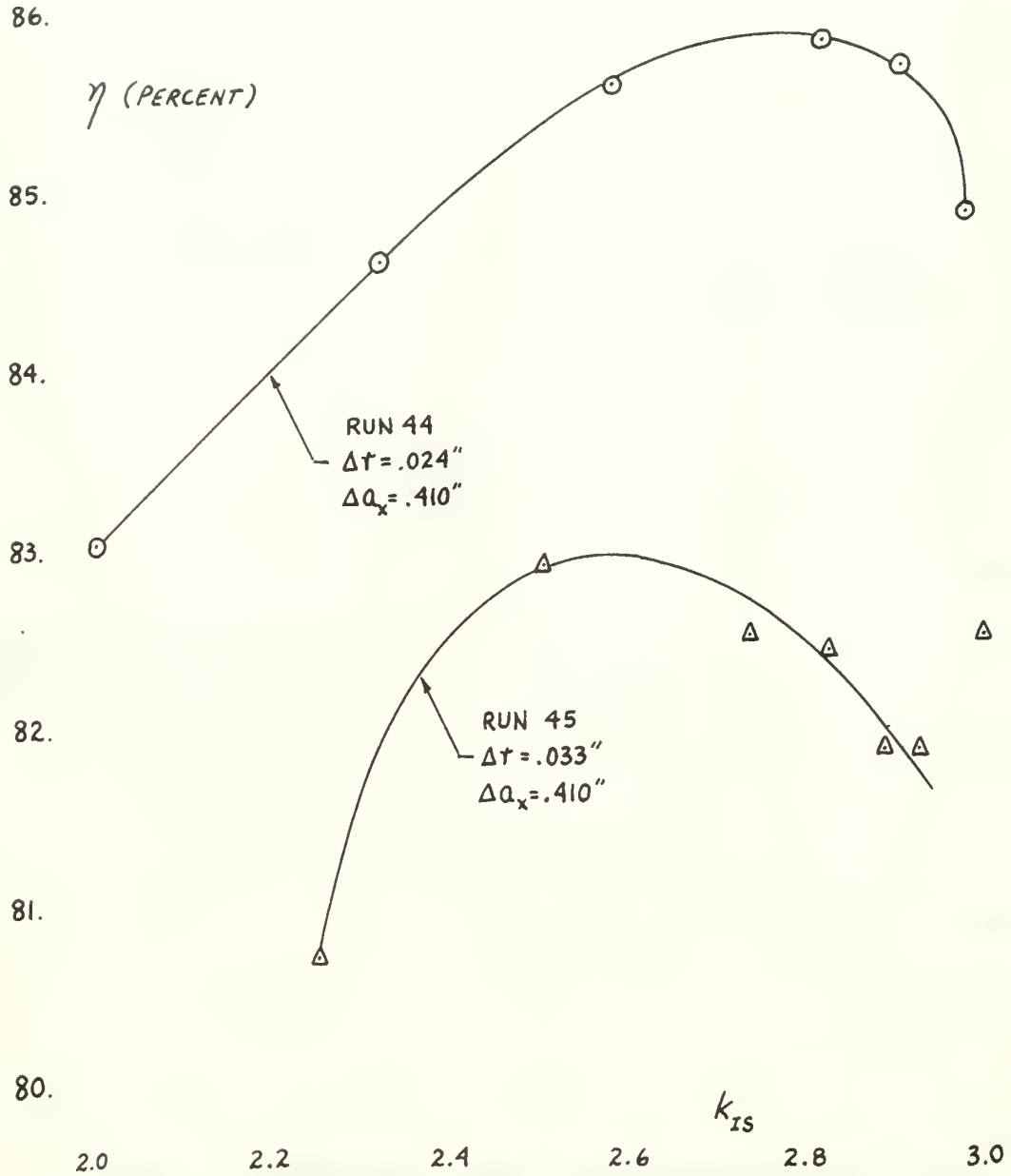

PLOT OF

TOTAL-STATIC EFFICIENCY VS ISENTROPIC HEAD COEFFICIENT

FOR THE MOD II ROTOR

AT $P_{T0}/P_2 = 1.3$

FIGURE 11

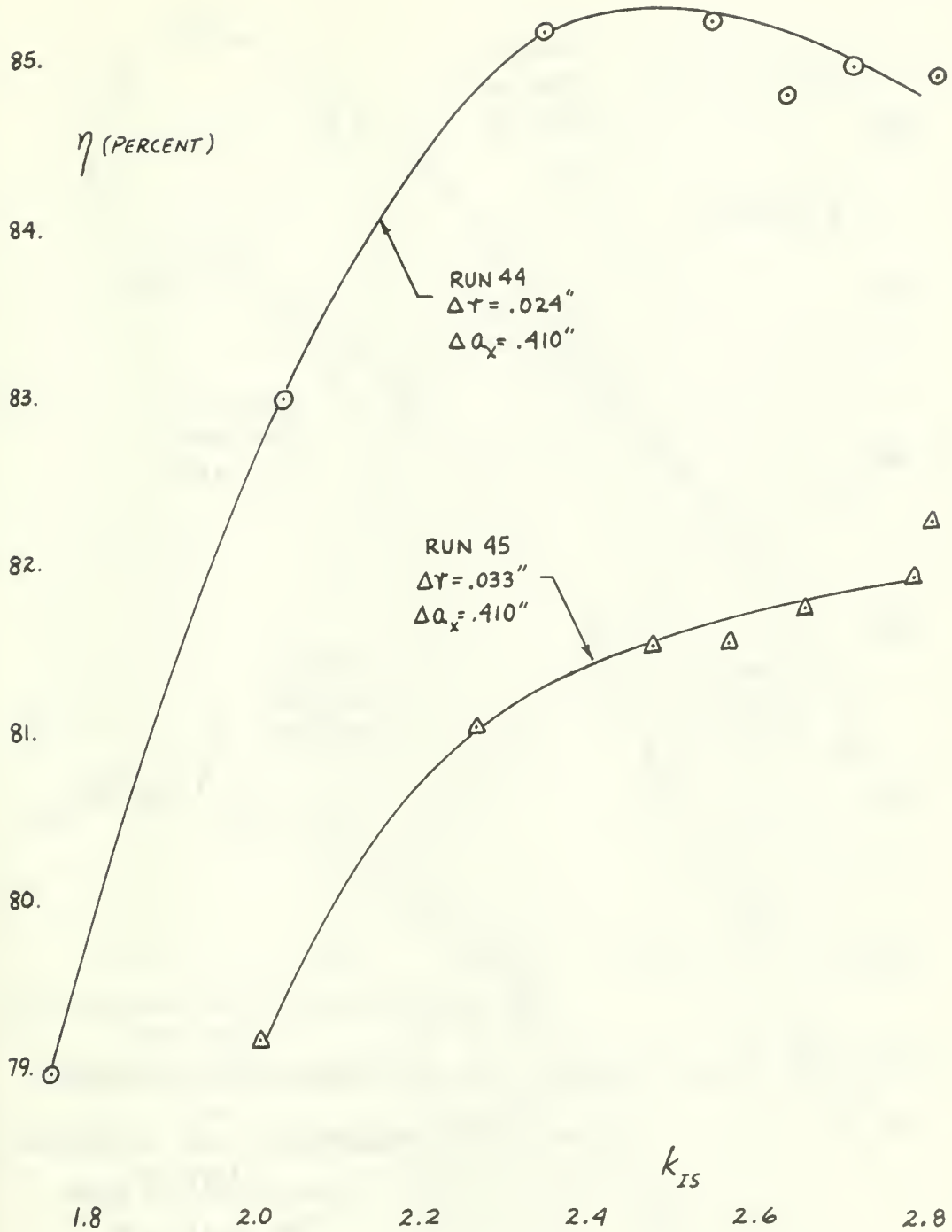

PLOT OF

TOTAL-STATIC EFFICIENCY VS ISENTROPIC HEAD COEFFICIENT

FOR THE MOD II ROTOR

$P_{T0}/P_2 = 1.4$

FIGURE 12

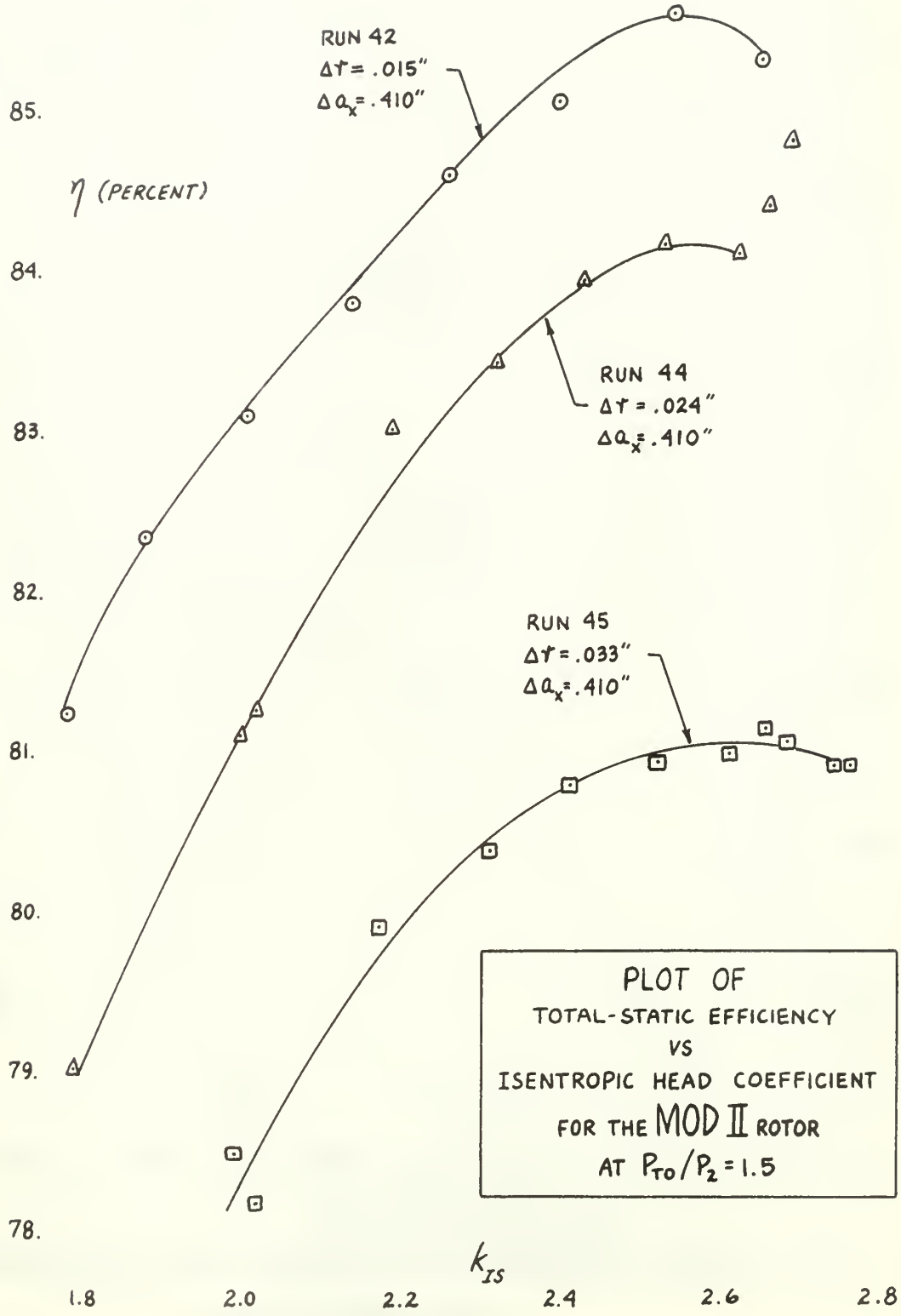
RUN 42
Δτ = .015"
ΔQx = .410"
RUN 44
Δτ = .024"
ΔQx = .410"
RUN 45
Δτ = .033"
ΔQx = .410"
η (PERCENT)
85.
84.
83.
82.
81.
80.
79.
78.
1.8
2.0
2.2
2.4
2.6
2.8
KIS
PLOT OF
TOTAL-STATIC EFFICIENCY
VS
ISENTROPIC HEAD COEFFICIENT
FOR THE MOD II ROTOR
AT PTO/P2 = 1.5

FIGURE 13

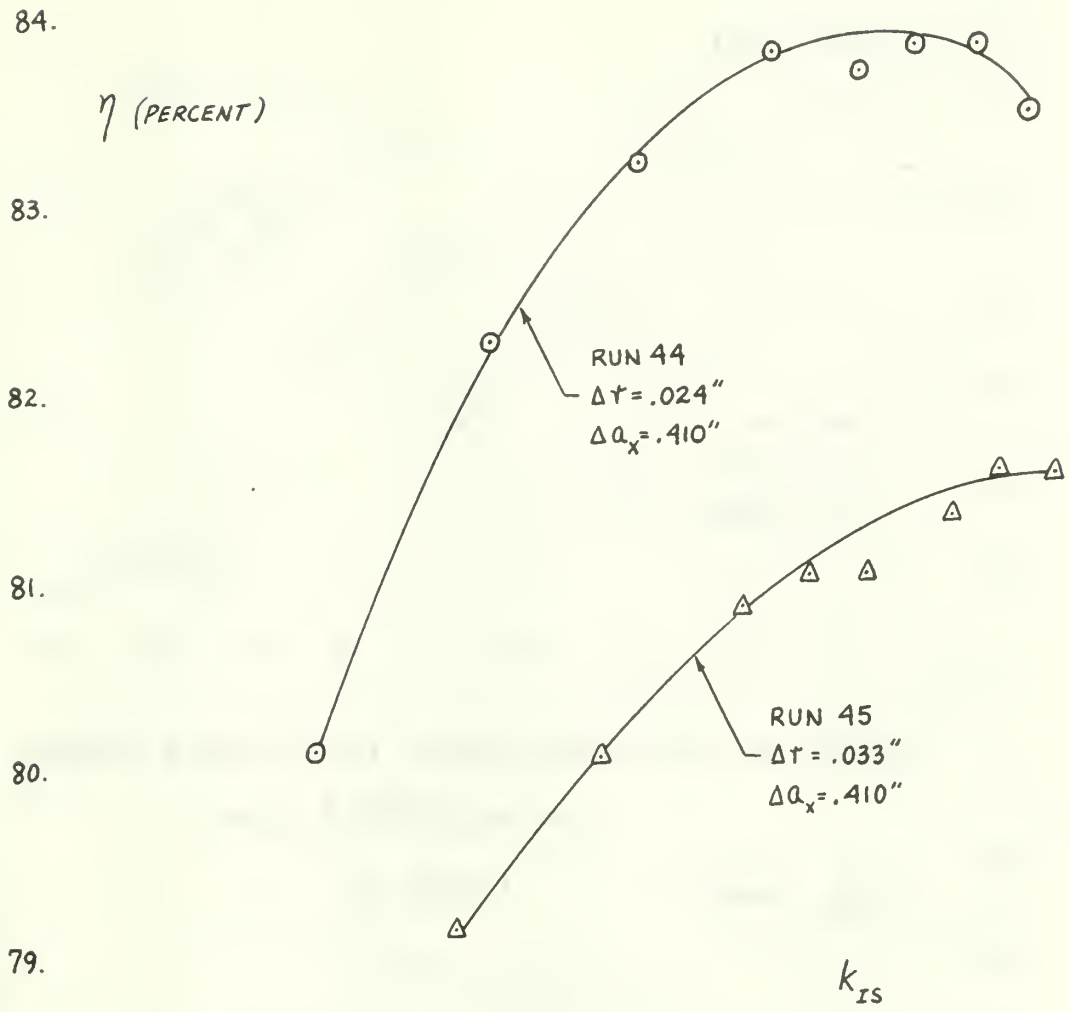

PLOT OF

TOTAL - STATIC EFFICIENCY VS ISENTROPIC HEAD COEFFICIENT

FOR THE MOD II ROTOR

AT $P_{T0}/P_2 = 1.55$

FIGURE 14

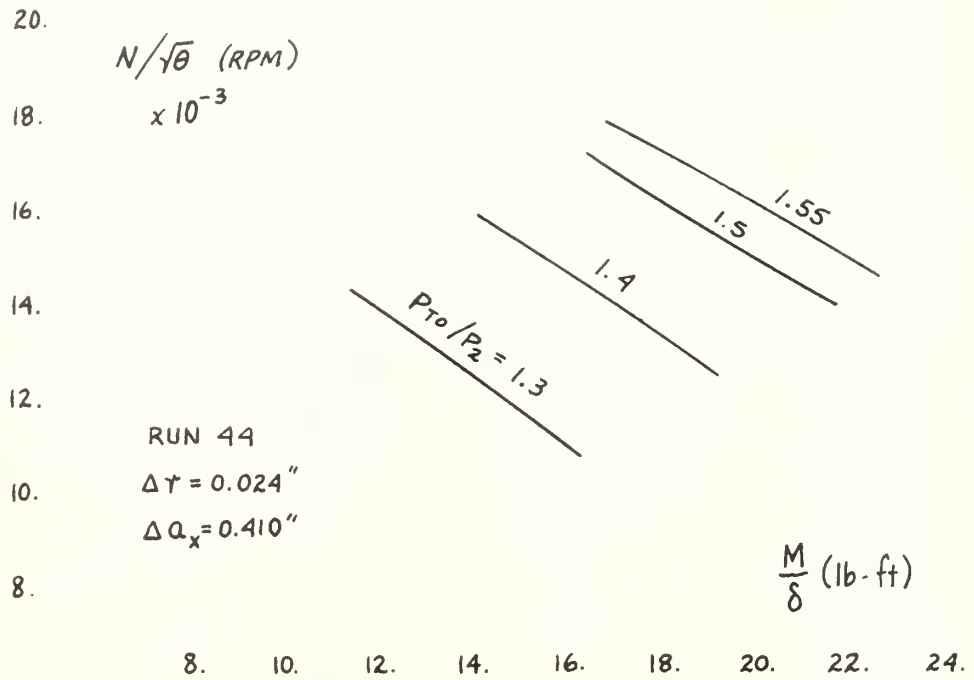

PLOTS OF REFERRED SPEED VS REFERRED TORQUE
FOR THE MOD II ROTOR
FIGURE 15

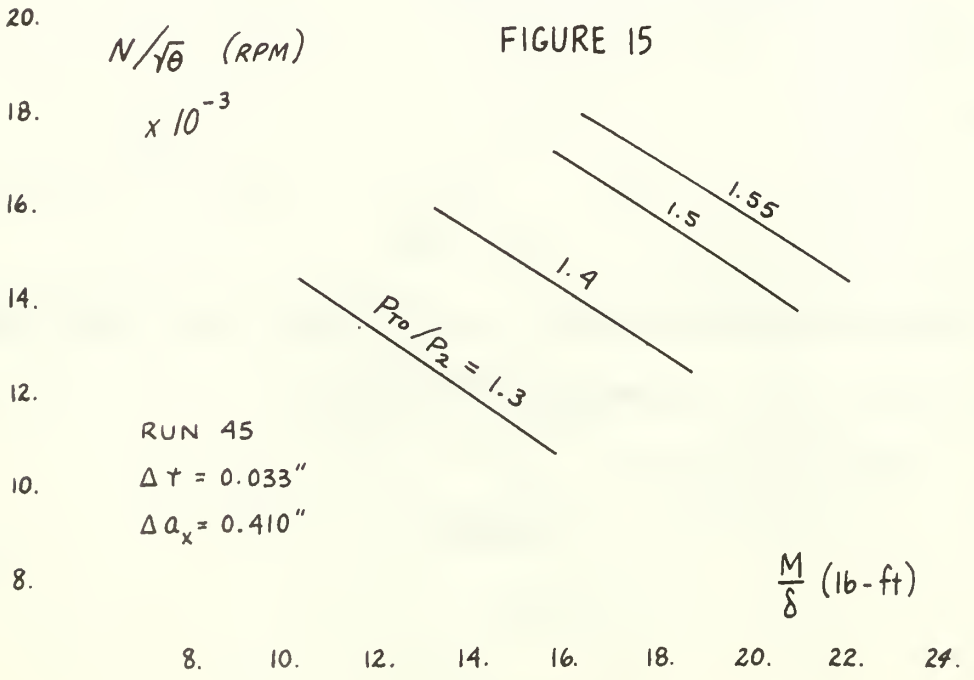

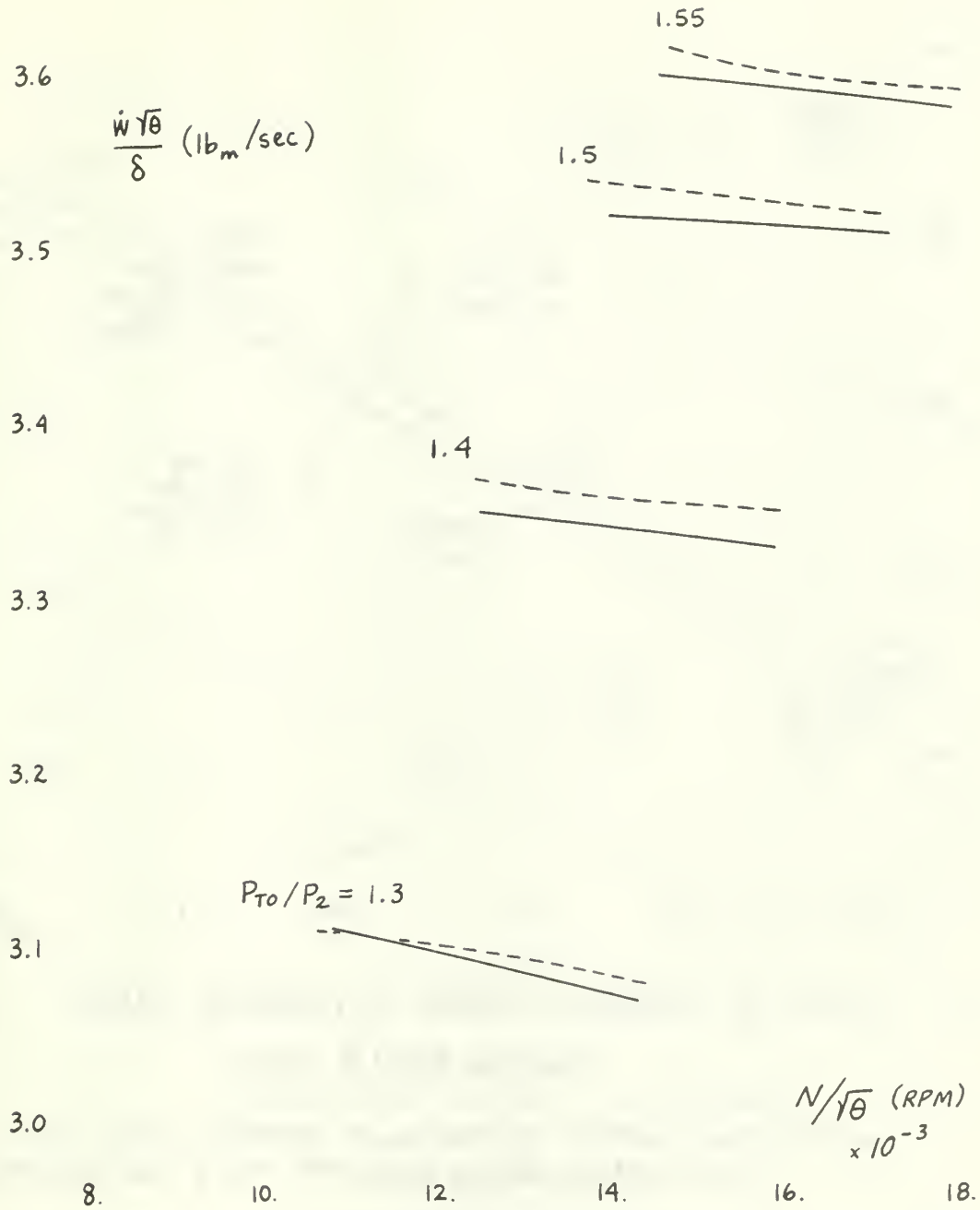

PLOT OF REFERRED FLOW RATE VS REFERRED SPEED

FOR THE MOD II ROTOR

RUN 44

$\Delta r = .024''$, $\Delta a_x = .410''$ ————

RUN 45

$\Delta r = .033''$, $\Delta a_x = .410''$ – – – – –

FIGURE 16

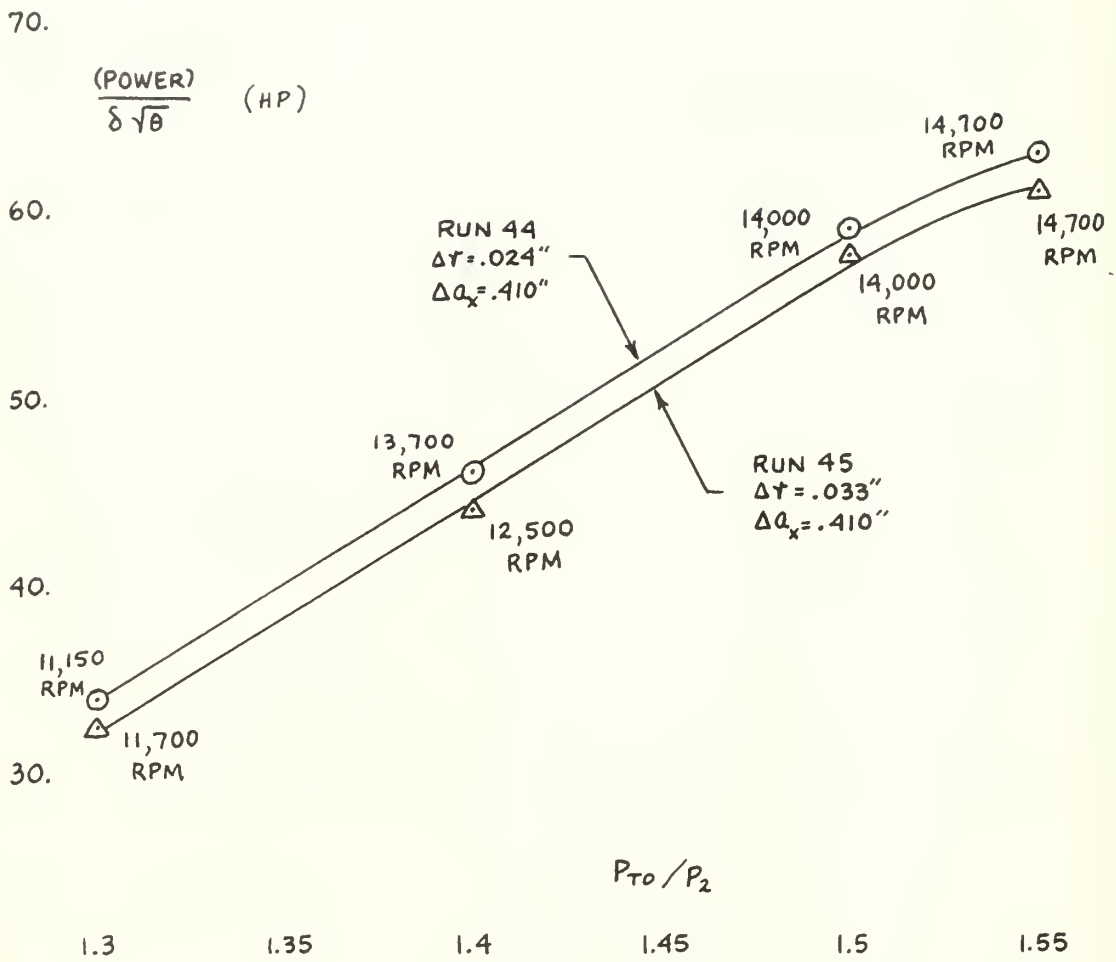

PLOT OF REFERRED POWER VS PRESSURE RATIO

FOR THE MOD II ROTOR

NOTE : "PEAK" POWER AT THE PARTICULAR PRESSURE RATIO IS THE VALUE PLOTTED, AND THE ASSOCIATED RPM IS ALSO INDICATED.

FIGURE 17

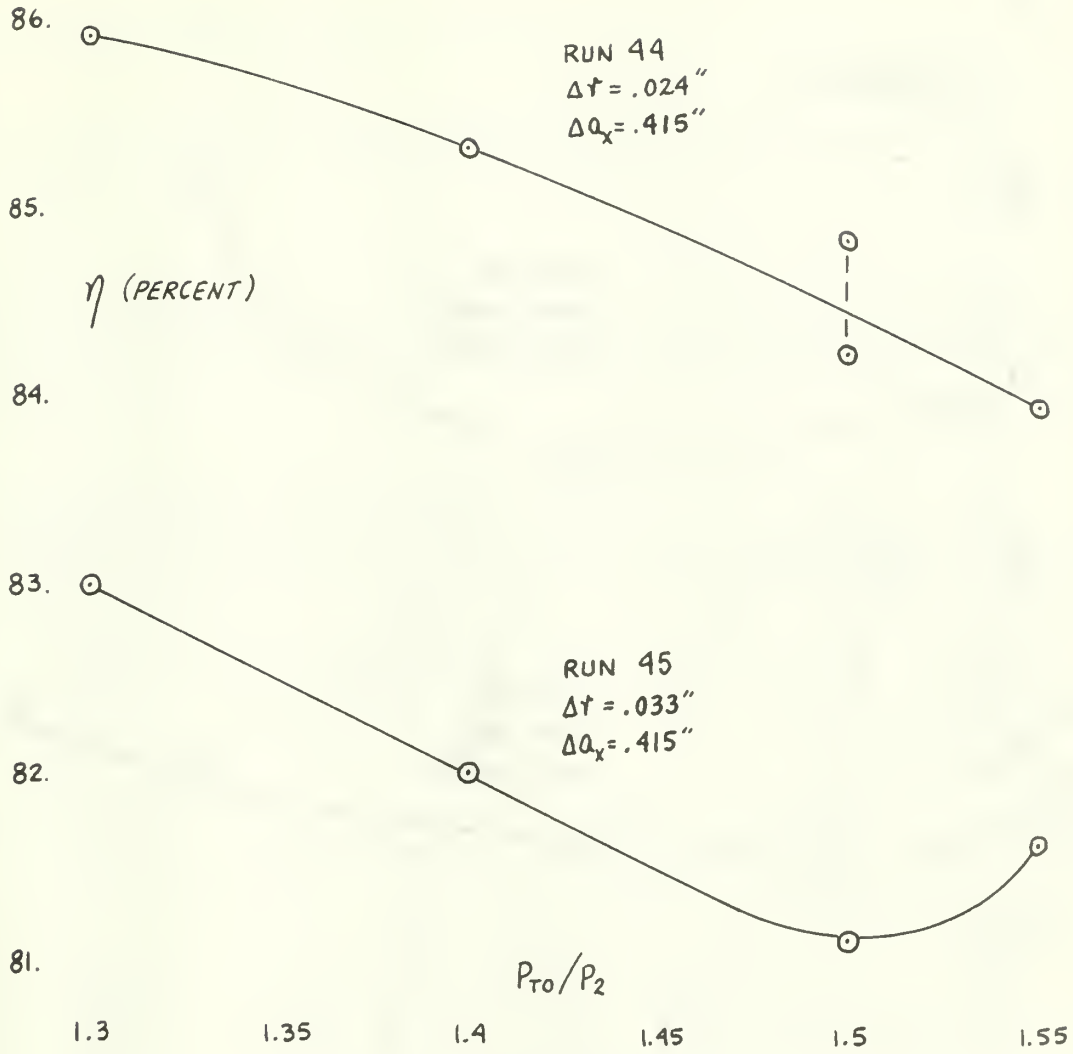

PLOT OF
PEAK TOTAL - STATIC EFFICIENCY
VS
PRESSURE RATIO
FOR THE MOD II ROTOR

FIGURE 18

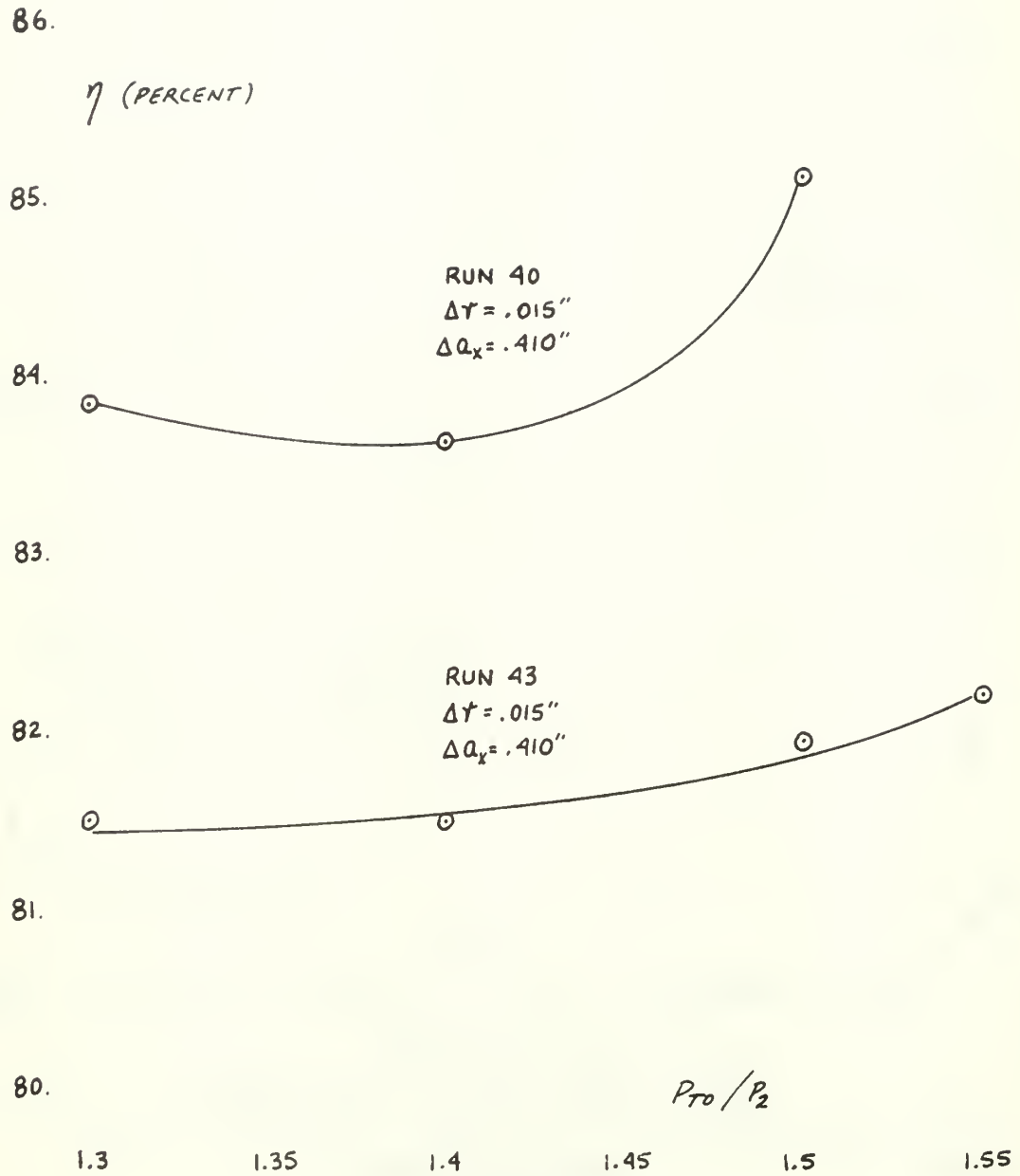

PLOT OF
PEAK TOTAL-STATIC EFFICIENCY VS PRESSURE RATIO
FOR THE MOD II ROTOR

FIGURE 19

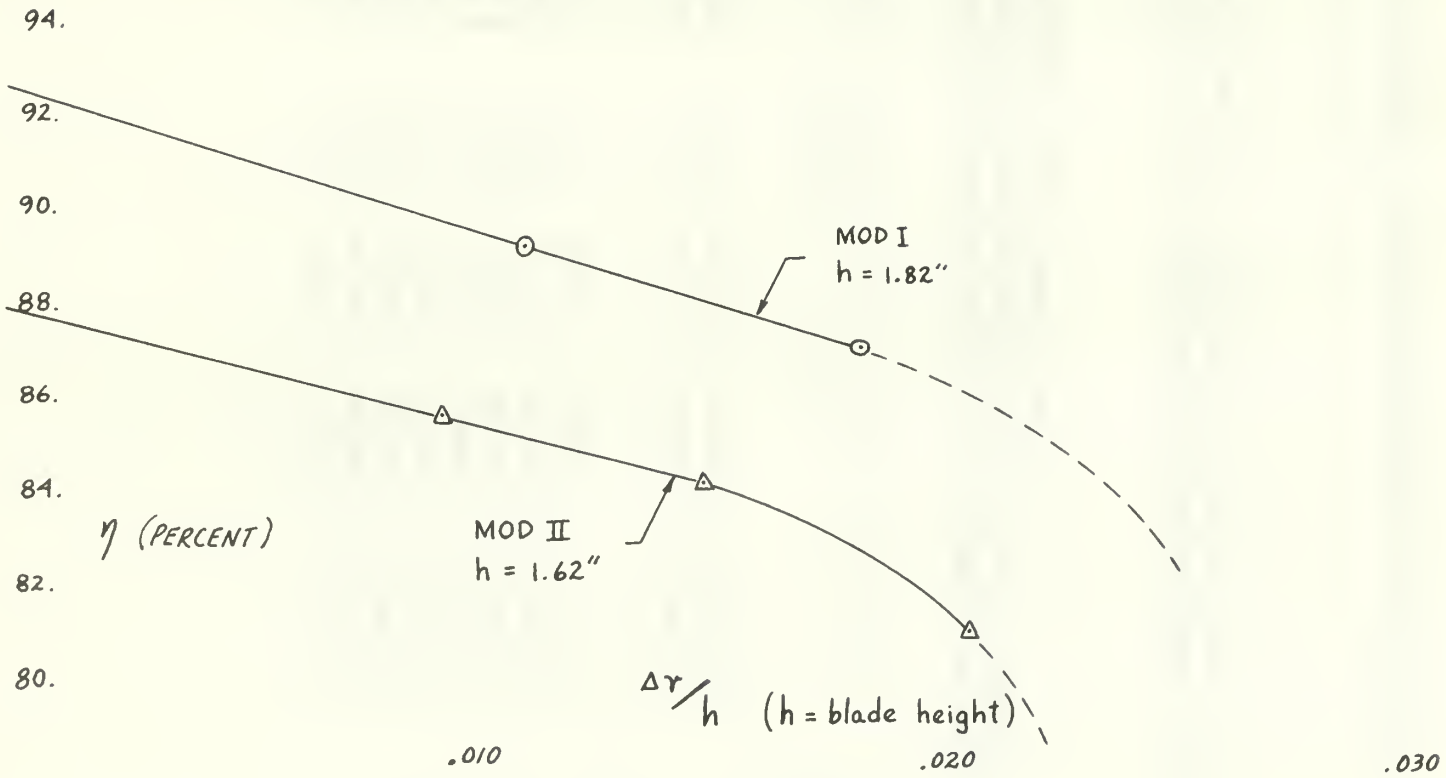

PLOT OF TOTAL-STATIC EFFICIENCY VS REFERRED RADIAL CLEARANCE FOR THE MOD I AND MOD II ROTORS

FIGURE 20

TABLE

TURBO - PROPULSION LABORATORY

OPERATING PERFORMANCE OF TURBINE STAGE FOR

TURBINE

ALPHA1 = 70. DEG., FLOW RESTRICTION FACTOR STATOR = .960
BETA2 = -63. DEG., FLOW RESTRICTION FACTOR ROTOR = .954
D1 = 8.25 IN.

FIRST LINE GIVES PERFORMANCE AT
SECOND LINE GIVES EQUIVALENT PERFORMANCE FOR
FOLLOWING LINES GIVE EQUIVALENT PERFORMANCE FOR

GAMMA	V1EQ	U1EQ	BETA1 (DEG)	PT0/P2	WF0EQ (SQ. IN)
1.2572	.66000	.57191	12.07	1.5108	6.8288
1.4010	.66000	.57191	12.07	1.4993	6.9096
1.4010	.45875	.39752	12.07	1.2000	5.3032
1.4010	.54422	.47158	12.07	1.3000	6.0562
1.4010	.60906	.52777	12.07	1.4000	6.5585
1.4010	.63613	.55123	12.07	1.4500	6.7499
1.4010	.66035	.57221	12.07	1.5000	6.9119
1.4010	.68203	.59100	12.07	1.5500	7.0494
1.4010	.70158	.60794	12.07	1.6000	7.1672
1.4010	.73514	.63702	12.07	1.7000	7.3560

III

USNPGS MONTEREY, CALIF.

GAMMA = 1.4010 FOR DESIGN CONDITIONS AT GAMMA = 1.2572

TYPE ARES MOD II

LOSS COEFF. STATOR = .079, THROAT AREA STATOR = 12.70 SQ.IN
LOSS COEFF. ROTOR = .093, THROAT AREA ROTOR = 16.08 SQ.IN
R2/R1 = .990

DESIGN CONDITIONS FOR GAMMA = 1.2572
GAMMA = 1.4010 AT SAME EQUIVALENT VELOCITY V1EQ
SAME ANGLES ALPHA1 AND BETA1 AT SELECTED PRESS. RATIOS

KIS	EFFIC. (PCT.)	DEGREE REACTION	ALPHA2 (DEG)	W1EQ	W2EQ	LEAV. LOSS COEFF.
2.5274	81.94	.4279	5.89	.23084	.61497	.0918
2.4841	82.08	.4179	7.93	.23084	.60839	.0910
2.3161	82.11	.3757	17.21	.16045	.38530	.0898
2.3692	82.15	.3897	14.11	.19034	.47149	.0897
2.4254	82.14	.4038	11.00	.21302	.54436	.0901
2.4542	82.12	.4108	9.47	.22249	.57745	.0905
2.4843	82.08	.4179	7.92	.23096	.60876	.0910
2.5158	82.03	.4252	6.35	.23855	.63883	.0917
2.5471	81.97	.4323	4.84	.24538	.66737	.0925
2.6142	81.80	.4469	1.78	.25712	.72183	.0944

TABLE

TURBO-PROPULSION LABORATORY

OPERATING PERFORMANCE OF TURBINE STAGE FOR

TURBINE TYPE ARES MOD II

ALPHA1 = 70. DEG., FLOW RESTRICTION FACTOR STATOR = .960
BETA2 = -63. DEG., FLOW RESTRICTION FACTOR ROTOR = .954
D1 = 8.25 IN.

MEASURED DATA ..PT0/P2=1.4980, WF0EQ = 6.8955 SQ. IN.

FIRST LINE GIVES PERFORMANCE CALCULATED FOR
SECOND LINE GIVES EQUIVALENT PERFORMANCE FOR
FOLLOWING LINES GIVE EQUIVALENT PERFORMANCE FOR

GAMMA	V1EQ	U1EQ	BETA1 (DEG)	PT0/P2	WF0EQ (SQ.IN)
1.4010	.66000	.57191	12.07	1.4993	6.9096
1.2572	.66000	.57191	12.07	1.5108	6.8288
1.2572	.45750	.39644	12.07	1.2000	5.2633
1.2572	.54188	.46955	12.07	1.3000	5.9909
1.2572	.60547	.52466	12.07	1.4000	6.4690
1.2572	.63180	.54747	12.07	1.4500	6.6486
1.2572	.65525	.56780	12.07	1.5000	6.7994
1.2572	.67619	.58594	12.07	1.5500	6.9265
1.2572	.69494	.60219	12.07	1.6000	7.0344
1.2572	.72678	.62977	12.07	1.7000	7.2048

IV

USNPGS MONTEREY, CALIF.

GAMMA = 1.2572 FROM TEST DATA WITH AIR AT GAMMA = 1.4010

TEST RUN 47 DATE 10/18/66 TEST POINT 7

LOSS COEFF. STATOR = .079, THROAT AREA STATOR = 12.70 SQ.IN.
LOSS COEFF. ROTOR = .093, THROAT AREA ROTOR = 16.08 SQ.IN.
R2/R1 = .990

KIS = 2.5816, EFFIC. = 80.64 PCT., DEGREE REACTION = .3989

AIR (GAMMA = 1.4010) WITH ABOVE LISTED INPUT DATA
GAMMA = 1.2572 AT SAME EQUIVALENT VELOCITY V1EQ
SAME ANGLES ALPHA1 AND BETA1 AT SELECTED PRESS. RATIOS

KIS	EFFIC. (PCT.)	DEGREE REACTION	ALPHA2 (DEG)	W1EQ	W2EQ	LEAV. LOSS COEFF.
2.4841	82.08	.4179	7.93	.23084	.60839	.0910
2.5274	81.94	.4279	5.89	.23084	.61497	.0918
2.3270	82.09	.3786	16.61	.16001	.38511	.0897
2.3872	82.11	.3943	13.17	.18952	.47120	.0898
2.4513	82.06	.4101	9.71	.21177	.54396	.0904
2.4847	82.02	.4180	8.00	.22098	.57694	.0909
2.5202	81.95	.4262	6.25	.22918	.60851	.0917
2.5558	81.88	.4342	4.54	.23650	.63832	.0925
2.5934	81.78	.4424	2.82	.24306	.66713	.0936
2.6727	81.53	.4590	-.59	.25420	.72168	.0962

BIBLIOGRAPHY

1. Eckert, R. H., Performance Analysis and Initial Tests of a Transonic Turbine Test Rig. USNPGS Thesis, May 1966.

2. Eckert, R. H., Determination of Flow Rates, Transonic Turbine Test Rig. USNPGS TN 66T-1, January 1966.

3. Naviaux, J. C., Transonic Turbine Test Rig Exhauster Tests, and Tests of a Reaction Turbine. USNPGS Thesis December 1966.

4. Vavra, M. H., Aero-Thermodynamics and Flow in Turbo-Machines, New York, London: John Wiley and Sons, Inc., 1960.

5. Vavra, M. H., Problems of Fluid Mechanics in Radial Turbomachines parts I & II. Von Karman Institute Course Note 55a. Rhode-Saint-Genese, Belgium: Von Karman Institute for Fluid Dynamics, March 1965.

6. Vavra, M. H., Problems of Fluid Mechanics in Radial Turbomachines parts III and IV. Von Karman Institute Course Note 55b. Rhode-Saint-Genese, Belgium: Von Karman Institute for Fluid Dynamics, March 1965.

7. Vavra, M. H., Determination of Single Stage Turbine Performance at Different Specific Heat Ratios. Unpublished notes, August 1966.

INITIAL DISTRIBUTION LIST

		No. Copies
1.	Defense Documentation Center Cameron Station Alexandria, Virginia 22314	20
2.	Library U. S. Naval Postgraduate School Monterey, California 93940	2
3.	Commander, Naval Air Systems Command Navy Department Washington, D. C. 20360	1
4.	Chairman, Department of Aeronautics U. S. Naval Postgraduate School Monterey, California 93940	2
5.	Professor M. H. Vavra Department of Aeronautics U. S. Naval Postgraduate School Monterey, California 93940	3
6.	LT. M. W. Wallace VFP 63 NAS Miramar, California 92145	2

UNCLASSIFIED

Security Classification

DOCUMENT CONTROL DATA - R&D

(Security classification of title, body of abstract and indexing annotation must be entered when the overall report is classified)

1. ORIGINATING ACTIVITY *(Corporate author)* U. S. Naval Postgraduate School Monterey, California	2a. REPORT SECURITY CLASSIFICATION 2b. GROUP

3. REPORT TITLE

PERFORMANCE ANALYSIS OF TWO REACTION TURBINES

4. DESCRIPTIVE NOTES *(Type of report and inclusive dates)*

Thesis

5. AUTHOR(S) *(Last name, first name, initial)*

WALLACE, Michael W., LT USN

6. REPORT DATE	7a. TOTAL NO. OF PAGES	7b. NO. OF REFS
December 1966	64	7

8a. CONTRACT OR GRANT NO.	9a. ORIGINATOR'S REPORT NUMBER(S)
b. PROJECT NO.	
c.	9b. OTHER REPORT NO(S) *(Any other numbers that may be assigned this report)*

14. KEY WORDS	LINK A		LINK B		LINK C	
	ROLE	WT	ROLE	WT	ROLE	WT
Transonic Turbine, USNPGS Monterey, Calif.						

INSTRUCTIONS

1. ORIGINATING ACTIVITY: Enter the name and address of the contractor, subcontractor, grantee, Department of Defense activity or other organization *(corporate author)* issuing the report.

2*a*. REPORT SECURITY CLASSIFICATION: Enter the overall security classification of the report. Indicate whether "Restricted Data" is included. Marking is to be in accordance with appropriate security regulations.

2*b*. GROUP: Automatic downgrading is specified in DoD Directive 5200.10 and Armed Forces Industrial Manual. Enter the group number. Also, when applicable, show that optional markings have been used for Group 3 and Group 4 as authorized.

3. REPORT TITLE: Enter the complete report title in all capital letters. Titles in all cases should be unclassified. If a meaningful title cannot be selected without classification, show title classification in all capitals in parenthesis immediately following the title.

4. DESCRIPTIVE NOTES: If appropriate, enter the type of report, e.g., interim, progress, summary, annual, or final. Give the inclusive dates when a specific reporting period is covered.

5. AUTHOR(S): Enter the name(s) of author(s) as shown on or in the report. Enter last name, first name, middle initial. If military, show rank and branch of service. The name of the principal author is an absolute minimum requirement.

6. REPORT DATE: Enter the date of the report as day, month, year; or month, year. If more than one date appears on the report, use date of publication.

7*a*. TOTAL NUMBER OF PAGES: The total page count should follow normal pagination procedures, i.e., enter the number of pages containing information.

7*b*. NUMBER OF REFERENCES: Enter the total number of references cited in the report.

8*a*. CONTRACT OR GRANT NUMBER: If appropriate, enter the applicable number of the contract or grant under which the report was written.

8*b*, 8*c*, & 8*d*. PROJECT NUMBER: Enter the appropriate military department identification, such as project number, subproject number, system numbers, task number, etc.

9*a*. ORIGINATOR'S REPORT NUMBER(S): Enter the official report number by which the document will be identified and controlled by the originating activity. This number must be unique to this report.

9*b*. OTHER REPORT NUMBER(S): If the report has been assigned any other report numbers *(either by the originator or by the sponsor)*, also enter this number(s).

10. AVAILABILITY/LIMITATION NOTICES: Enter any limitations on further dissemination of the report, other than those imposed by security classification, using standard statements such as:

(1) "Qualified requesters may obtain copies of this report from DDC."

(2) "Foreign announcement and dissemination of this report by DDC is not authorized."

(3) "U. S. Government agencies may obtain copies of this report directly from DDC. Other qualified DDC users shall request through _____."

(4) "U. S. military agencies may obtain copies of this report directly from DDC. Other qualified users shall request through _____."

(5) "All distribution of this report is controlled. Qualified DDC users shall request through _____."

If the report has been furnished to the Office of Technical Services, Department of Commerce, for sale to the public, indicate this fact and enter the price, if known.

11. SUPPLEMENTARY NOTES: Use for additional explanatory notes.

12. SPONSORING MILITARY ACTIVITY: Enter the name of the departmental project office or laboratory sponsoring *(paying for)* the research and development. Include address.

13. ABSTRACT: Enter an abstract giving a brief and factual summary of the document indicative of the report, even though it may also appear elsewhere in the body of the technical report. If additional space is required, a continuation sheet shall be attached.

It is highly desirable that the abstract of classified reports be unclassified. Each paragraph of the abstract shall end with an indication of the military security classification of the information in the paragraph, represented as *(TS)*, *(S)*, *(C)*, *or (U)*.

There is no limitation on the length of the abstract. However, the suggested length is from 150 to 225 words.

14. KEY WORDS: Key words are technically meaningful terms or short phrases that characterize a report and may be used as index entries for cataloging the report. Key words must be selected so that no security classification is required. Identifiers, such as equipment model designation, trade name, military project code name, geographic location, may be used as key words but will be followed by an indication of technical context. The assignment of links, roles, and weights is optional.

DD FORM 1 JAN 64 1473 (BACK)